

---

# Introduction

*One of the most conspicuous properties of nature is the great diversity of size and length scales in the structure of the world. An ocean, for example, has currents that persist for thousands of kilometers and has tides of global extent; it has also waves that range in size from less than a centimeter to several meters; at much finer resolution, seawater must be regarded as an aggregate of molecules whose characteristic scale of length is roughly  $10^{-8}$  centimeters. From the smallest structure to the largest is span of 17 orders of magnitude. In general, events distinguished by great disparity in size have little influence on one another; they do not communicate, and so the phenomena associated to each scale can be treated independently. The interaction of two adjacent molecules is much the same whether the molecules are in the Pacific Ocean or in a teapot. What is equally important, an ocean wave can be described quite accurately as a disturbance of a continuous fluid, ignoring completely the molecular structure of the liquid. The success of almost all practical theories in physics depends on isolating some limited range of length scales. If it were necessary in the equation of hydrodynamics to specify the motion of every water molecule, a theory of ocean waves would be far beyond the means of the 20th century science. A class of phenomena does exist, however, where events at many scales of length make contributions of equal importance. An example is the behaviour of the water when it is heated to boiling under the pressure of 217 atmospheres. At that pressure water does not boil until the temperature reaches 647 degrees Kelvin. This combination of pressure and temperature defines the critical point of water, where the distinctions between fluid and gas disappear; at higher pressures there is just a single, undifferentiated fluid phase, and water cannot be made to boil no matter how much the temperature is raised. Near the critical point water develops fluctuations in density at all possible scales. The fluctuations take the form of drops of liquid thoroughly interspersed with bubbles of gas, and there are both drops and bubbles of all sizes from the single molecules up to the volume of the specimen. Precisely at*

*the critical point, the length scale of the largest fluctuations becomes infinite, but the smaller fluctuations are in no way diminished. Any theory that describes a system near its critical point must take into account the entire spectrum of length scales.*

K.G. Wilson [Wil79]

## 1.1 What is complexity?

The term *complexity* is probably one of the most intuitive and, at the same time, elusive in modern science. Although a precise definition is lacking, nevertheless, everybody can imagine a complex system to be just something that it is hard to understand! This, of course, is not very rigorous. An example would probably help to clarify this concept. Suppose we have an unspecified device, a “black box”, that we want to analyze. In order to have some insight into its behaviour, it is natural to supply it with some kind of linear input and then look at the results. If the output obtained is nothing that can be easily foreseen from the knowledge of the initial condition that we imposed, then we can start arguing that what we are dealing with is something “complex”. This simple example points out, possibly, the most outstanding benchmark of all the complex systems, that is the **non-linearity** of the forces acting between elementary parts composing the system itself. These kinds of interactions usually lead to the **emergence** of patterns which are considered to be another peculiarity of complex systems.

However, non-linearities and emergent behaviour are not the only symptoms of complexity, rather they are just the tip of the iceberg. Other characteristic features include:

- **Feedback:** Both negative (damping) and positive (amplifying) are typically encountered in complex systems. The stock market is a clear example: previous trades can have repercussions on current decisions. Memory effects can also lead to **hysteresis** phenomena.
- **Non-equilibrium:** Complex systems in nature are usually open, dissipative, systems. Nevertheless, patterns of stability can be found.
- **Embedded complexity:** The components of a complex system may themselves be complex systems. For example, an economy is made up of organizations, which are made up of people, which are made up of cells - all of which are complex systems.
- **Multifractal/multiscale processes:** Usually, the dynamics of complex

systems involves different temporal and spatial scales, giving rise to self-similar features.

- **Network of interactions:** The topology of the interactions between the parts of these systems is often described by non-trivial networks.
- **Self-organization:** Complex systems often tend to *self*-organize and give rise to coherent structures without external inputs. A broader discussion on this argument is given in Chapter 2.

Now that we have a vague idea of what we are dealing with, we can start wondering: is there any chance to predict the behaviour of these systems? Although this question may sound academic, it is everything but. **Predictability** is probably the most outstanding issue in complex system theory. Most complex systems, in fact, are not found in an exotic physics laboratory, but they are actually related to many common aspects of every-day life. Most people would be surprised to know, for example, that there are emergent patterns in traffic jams or how the dynamics of earthquakes and the stock market have similarities during specific periods, as shown in Fig. 1.1. No need to say that the capability to predict, even for very short horizons, the behaviour of these systems would be a great step forward for human society. To some extent, the degree of predictability itself can be used to define *how* complex the system is [BCFV02].

At this point, I hope the reader has a general idea regarding the main features characterizing a complex system. A more detailed and advanced introduction, that goes beyond the scope of this work, can be found in the book of Badii and Politi [BP97]. In order to have a better overview of the subject, in the next section we introduce complexity from an historical prospective and, after that, we consider some specific examples of complex systems.

## 1.2 Complexity: an historical overview

As a matter of fact the the world is not simple! Our prehistoric ancestors already realized how complex it is to start a fire to cook the meat! So, is there any possibility of tracking back the origin of complexity without getting lost in the sands of time? In reality there is, as long as we realize that “complex problems” are not “complex systems”: while the latter are defined inside a scientific framework, the former belong to the sphere of philosophy and must not be addressed in this context.

After this preface, we can say that modern *complex system theory*, as an independent area of research dates back to the early '80s, and, precisely, in May

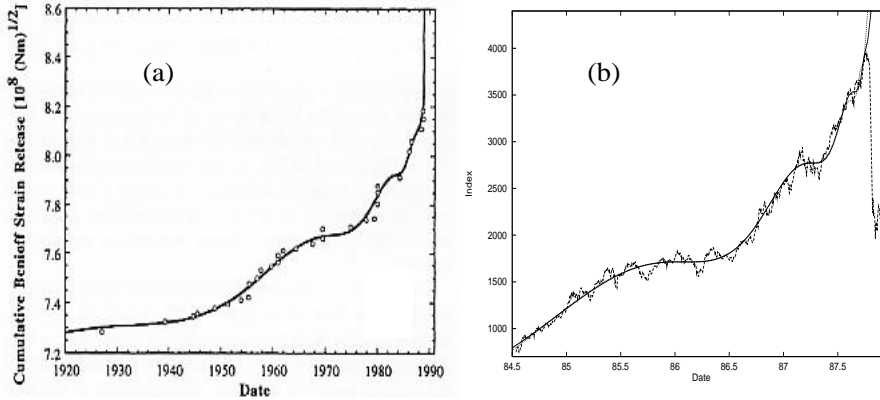


Figure 1.1: (a) Cumulative Benioff strain release in magnitude 5 or greater earthquakes in the San Francisco Bay area before the 17th October 1989 Loma Prieta earthquake [NTG95]. (b) Hang Seng index for the Hong Kong stock market prior to the 1994 crash [Sor03b]. Both data sets are fitted with a log-periodic function, derived by a possible underlying *discrete scale invariance* in these two different systems. A more exhaustive discussion on the subject can be found in Chapter 2.

1984, with the foundation, by George Cowan, of the Santa Fe Institute. Two years later, the Center for Complex Systems at the University of Illinois, led by Stephen Wolfram, become operative as well. The rise of these two institutions, explicitly devoted to the interdisciplinary study of complex phenomena, can arguably be considered as the dawn for complex system research as we know it today.

However, already at the end of the 19th century the notion of complexity, and non-predictability in particular, started to become familiar to the scientific community as the result of the independent works of the Austrian physicist Ludwig Boltzmann and the French mathematician Henri Poincaré.

Ludwig Boltzmann, the father of *statistical mechanics*, raised, for the first time in modern physics, important arguments against determinism, in a Newtonian sense, of the dynamics of systems composed by many interacting elements, as, for example, a gas. The statistical approach that Boltzmann introduced to overcome this problem was a great success. Dropping the standard equations of motion, all the physics of the system was determined by just three parameters: temperature, volume and pressure. On the other hand, Henri Poincaré, during the 1890s, proved that the motion of three planets influenced only by the gravitational (non-linear) forces acting between them, could be extremely com-

plicated and, actually, unpredictable. The *three body problem* to some extent, can be considered as a precursor of *chaos theory*.

These discoveries had a great impact on the scientific community of that age. In fact, most of the physicists used to share the same beliefs as Newton, that is, the complexity of the world was just apparent: once the physical laws describing it were discovered, then the ordered pattern of Nature should have appeared as well. Statistical mechanics and non-linear dynamics, for the first time, question this vision: the single parts do not add up and there is an intrinsic complexity and unpredictability in the world which, actually, seemed to tend toward a disordered state.

After Boltzmann and Poincaré, different scientists faced problems that, today, we could call “complex”. Nevertheless, in order to have a coherent movement which recognized the intrinsic importance of complexity we have to wait until the late 1940s. The reason for this lies in the fact that complexity was, and still is, deeply related with computation and, therefore, with the development of computers and computer science.

In 1948, Claude E. Shannon founded the field of *information theory*, a mathematical framework for data communication and storage. It is actually in this context that complexity started to be regarded as a principal area of research. In this particular case, the issue with complexity was related to the minimum information that could completely describe a certain signal. In order to tackle this problem, Shannon defined a measure, known as *Shannon entropy* due to analogies with the definition of entropy in thermodynamics, which, when applied to an information source, could determine the minimum channel capacity required to reliably transmit the source as encoded binary digits. Historically, the *minimum information*, that is the number of bits describing the signal, became the first quantitative measure of *complexity*.

During these years, information theory developed in different directions. The problems explicitly regarding complexity were addressed in the branch called *computational complexity theory*, devoted to the study of the “resources” required during computation to solve a given problem. The main resources, in this case, were time (how many steps it would take to solve a problem) and space (how much memory it would take). In this area important progress was made in *defining* complexity in a formal way, as, for example, the *algorithmic complexity*, that is the size of the minimal program able to reproduce an input string (Solomonoff, 1964 [Sol64]; Kolmogorov, 1965 [Kol65]; Chaitin, 1966 [Cha66]).

Still, regarding the relation between complexity and computer science, it is worthy to mention the work of Alan Turing who, in 1936, developed the famous *Turing machine*, a theoretical computing device to serve as an idealized model for mathematical calculation [Tur36]. The idea of Turing, had important

repercussions in the future development of numerical models. In fact, it led to the introduction of one of the most popular tools able to represent the dynamical behaviour of extended complex systems, that is *cellular automata*, developed in the late 1940s by John von Neumann [vN66]. Cellular automata are discrete systems, both in space and time, in which the elementary cells evolve according to some local rules. This simulation method gained a vast popularity thanks to the *Game of Life* by John H. Conway (1970). In this model, several properties, similar to the ones of a microscopic “living” world, emerge by the application of a set of simple deterministic rules [BCG82]: soon it became a paradigm of the complex system. Further works in cellular automata, along with their applications in different areas of science, were carried on in the '80s by different authors and in particular Stephen Wolfram [Wol86].

Other areas in which the concept of complexity has been often associated are hydrodynamic turbulence and biological evolution (especially after the discovery of periods of mass extinction). These areas will be more specifically discussed in the next section.

This brief introduction on the historical background of complex system theory, far from being exhaustive, can give a idea to the reader how it is basically impossible to find a simple temporal path for the evolution of this multidisciplinary area which has roots in basically all the scientific disciplines. Its evolution has been highly non-linear through the time, but how could anyone have possibly expected anything less than that!

### 1.3 Example of complex systems: from physics to finance

The notion of complexity is not limited to some specific areas of human knowledge but rather embraces all possible fields of investigation. In the following subsections we give some examples of complex systems, selected from, apparently, very different disciplines such as physics (turbulence and spin glasses), biology (evolution of species) and economics (the stock market). These examples, although not exhaustive, can give a feeling to the reader of how broad complexity is and how much we still have to investigate in order to reach some decent understanding of the way things “work”.

### 1.3.1 Turbulence

Hydrodynamic turbulence is probably one of the most outstanding problems in modern physics and the difficulties in this field can be summarized by a famous aphorism from Sir Horace Lamb:

*When I die and go to Heaven there are two matters on which I hope enlightenment: one is quantum electrodynamics and the other is turbulence of fluids. About the former I am really rather optimistic.*

This sentence, although sarcastic, is definitely appropriate. After all, the physics of incompressible fluids, turbulence included, is contained in the Navier-Stokes equations,

$$\begin{aligned}\partial_t \vec{v} + (\vec{v} \cdot \vec{\nabla}) \vec{v} &= -\vec{\nabla} p + \nu \nabla^2 \vec{v}, \\ \vec{\nabla} \cdot \vec{v} &= 0,\end{aligned}\tag{1.1}$$

where  $\vec{v}$  is the velocity field of the flow,  $p$  is the pressure and  $\nu$  the kinematic viscosity. These equations are known since 1823 and, in principle, once we have defined the initial and boundary conditions, we should be able to solve the equation of motion, turbulence included. Unfortunately, this is true just theoretically. If we look at the experiments, we obtain a rich dynamics that is basically impossible to recover, for different technical reasons, by just integrating the Navier-Stokes equations.

The transition from an ordered, or quiescent, state in the fluid, where we have an homogeneous distribution of the velocity field, to a turbulent regime, where the velocity field becomes spatio-temporally chaotic, is due to the injection of energy at large scales, see Fig. 1.2 [Fri95]. In the so called *fully turbulent regime* several orders of length scales are involved in the process of energy transfer from the largest to the smaller ones, where the energy is finally dissipated. Actually, what we observed is an *energy cascade* where eddies of all sizes are active, as shown in the sketch of Fig. 1.2 (c) [Fri95]. Moreover, this property does not depend on the specific fluid under consideration: it is universal.

A very important parameter used in turbulence studies in order to characterize the state of the system is the *Reynolds number*,  $R_l$ , defined as  $R_l = v_l l / \nu$ , where  $v_l$  is the velocity difference at some scale  $l$ . This number characterizes the interplay between the nonlinear advection,  $(\vec{v} \cdot \vec{\nabla}) \vec{v}$ , and dissipation,  $\nu \nabla^2 \vec{v}$ , terms in Eq. (1.1). While the drag term tends to bring the fluid into a quiescent state, a high velocity field, enhanced by the injection of energy at large scales, tends to drive the fluid toward a turbulent state. In this phase the smallest eddies have a limiting size, called *Kolmogorov length*, of  $l_d = (\nu / \bar{\epsilon})^{1/4}$ , with  $\bar{\epsilon}$

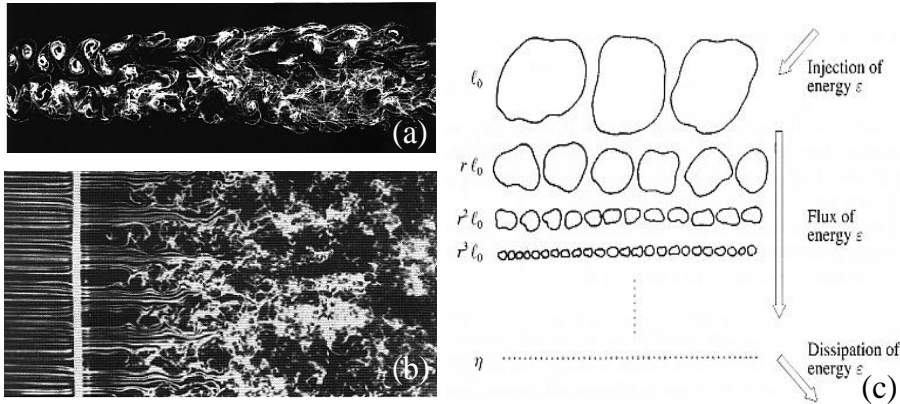


Figure 1.2: (a) Wake behind two identical cylinders at  $Re = 240$ . (b) Homogeneous turbulence behind a grid. (c) Space fillings eddies in a sketch of the Kolmogorov 1941 theory. In this case,  $l_0$  is the size of the largest eddies and  $r = 1/2$  is the scaling ratio. These pictures are taken from [Fri95].

being the mean dissipation rate. Each of the smallest eddies can be associated with the degrees of freedom,  $N_d$ , of the fluid and their number goes approximately as  $R^{9/4}$  per unit of volume. In order to give an insight into the problem, we can think about the turbulence in the atmosphere. In this case  $R > 10^{18}$  and, therefore, the degrees of freedom are greater than  $10^{45/2}$  per unit of volume! This kind of problem would discourage most people to attempt a large scale simulation of turbulence. In reality, there are empirical laws that seem to come to help. In fact the sizes of the eddies are not randomly distributed but they follow a self-similar hierarchy from the largest to the small scales until the dissipation takes over. This self-similarity property has led to the famous theory formulated by Kolmogorov in 1941. In this formulation the scaling exponent,  $\zeta_m$ , of the  $m$ -order structure function for the velocity field,

$$\langle |\vec{v}(\vec{x} + \vec{l}) - \vec{v}(\vec{x})|^m \rangle \sim |\vec{l}|^{\zeta_m}, \quad (1.2)$$

is supposed to scale as  $\zeta_m = m/3$ . The regime in which this condition is satisfied goes under the name of the *inertial regime*,  $l_d \ll l \ll l_s$ , where  $l_s$  is the size of the system. However, nonlinear deviations from this scaling behaviour have been experimentally found, leading to the formulation of different phenomenological models. An excellent general review on the subject of turbulence can be found in the seminal book of Frisch [Fri95] while for more a detailed discussions regarding the dynamical system approach and modeling we suggest the book of Bohr et al. [BJPV98].



At this point it is trivial to state that turbulence is a highly complex field due to the non-linearity and high dimensionality of the problem. Nevertheless, this high complexity gives rise to structures and emerging patterns at all scales, in a fashion similar to other systems with less degrees of freedom. Therefore, we need to find a representation, possible to handle from a computational point of view, which gives rise to the basic structures observed.

### 1.3.2 Complex systems in statistical mechanics: the spin glasses

In equilibrium statistical mechanics, systems gradually evolve toward the state of minimum energy where the fluctuations of the macroscopic variables eventually vanish. In general, the macroscopic properties of the system can be deduced from the Gibbs-Boltzmann assumption. In this framework each possible configuration of the system,  $X = (p_1, \dots, p_i, \dots, q_1, \dots, q_i, \dots)$ , fixes a certain weight,  $\exp[-H(X)/k_B T]$ , where  $H(X)$  represents the energy of the system in the state  $X$  at the temperature  $T$  and  $k_B$  is the Boltzmann constant. A faithful physical description is possible once we identify an ensemble of micro-states which give a leading contribution to the statistical averages for an infinite system size, that is in the *thermodynamic limit*. This correspondence is governed by the balance of the weights for the various configurations, controlled by the energy, and their number, quantified by the entropy.

An example of a statistical system governed by such a dynamics is the *Ising model*, where the evolution of a set of  $N$  boolean spins,  $\sigma_i = \pm 1$  ( $i = 1, \dots, N$ ), is described by the Hamiltonian,

$$H = - \sum_{ij} J_{ij} \sigma_i \sigma_j - \sum_i h_i \sigma_i, \quad (1.3)$$

where  $J_{ij}$  is the coupling constant between spins  $i$  and  $j$  and  $h_i$  is the strength of an external magnetic field. Due to the discreteness of its variables, the dynamics is not usually solved analytically but via numerical methods, such as *Monte Carlo* algorithms. In this case the evolution of the system is simulated stochastically by associating a transition probability,  $W(X \rightarrow \tilde{X})$ , corresponding to a spin flip, to switch from one configuration,  $X$ , to another,  $\tilde{X}$ . In practice, the coefficient  $W$ s satisfy the *detailed balance* condition

$$\frac{W(X \rightarrow \tilde{X})}{W(\tilde{X} \rightarrow X)} = \exp\left(-\frac{\Delta H}{k_B T}\right), \quad (1.4)$$

with  $\Delta H = \tilde{H}(X) - H(X)$ . This condition is imposed in a way that, at equilibrium, the number of transitions from the state  $X$  to  $\tilde{X}$  is balanced by the

number of transitions from  $\tilde{X}$  to  $X$ . A proper choice for  $W$  was suggested by Metropolis in 1953 [MRR<sup>+</sup>53] and it is still widely used. This rule reads

$$W(X \rightarrow \tilde{X}) = \begin{cases} 1 & \text{if } \Delta H < 0, \\ \exp(-\Delta H/k_B T) & \text{if } \Delta H > 0 \end{cases} \quad (1.5)$$

and it is known as *Metropolis algorithm*.

Although this formalism appears to be relatively simple, it can give rise to very complex dynamics. The source of complexity, in this case, is fixed by the energy landscape generated by the particular Hamiltonian under consideration. In fact, in some particular cases this landscape is not “smooth” but rough and organized in a hierarchical structure of local minima. In this case the system can get trapped in one of these minima and the exploration of the rest of the state-space can happen just sporadically. This “frozen state” is directly related to the problem of *ergodicity breaking*, that is the impossibility of accessing all the allowed configurations: the macroscopic state become dependent on the initial conditions.

The most popular example of spin systems showing ergodicity breaking and a complex energy landscape is the *spin glass*. Spin glasses, originally introduced to simulate the behaviour of alloys, such as CuMn, are magnetic systems, similar to the Ising model, in which there is “competition” between the interactions of the magnetic moments resulting in a frozen-in disorder reminiscent of what occurs in ordinary glass. Although these systems lack long range order, they are characterized by short range order below the spin glass temperature,  $T_f$ , when magnetic clusters starts to appear. In this case the complexity of the energy landscape emerges from the conflicting interests between spins, or *frustration*, and a certain degree of disorder in the interactions.

The simplest model of a spin glass is defined by the Hamiltonian in Eq. (1.3), where the interactions between spins,  $J_{ij}$ , are not uniformly ferromagnetic,  $J_{ij} = +1$ , or antiferromagnetic,  $J_{ij} = -1$ , but they are randomly distributed on the lattice. This simulates the intrinsic disorder of the material and leads to the random frustration of the cells. Moreover, we can set  $h_i \equiv 0$ .

The complexity of the energy landscape generated by spin glass models extended their application beyond the boundaries of solid state physics. An example is the dynamics of ecologies, where the evolution of species is supposed to take place in a rough landscape of energy, called *fitness*, similar to the one observed in spin glasses. Other relevant examples of interdisciplinary application of spin glasses can be found in optimization theory, neural networks, protein folding and social interactions. For a review on spin glass theory, the interested reader can have a look at Refs. [MPV87] and [BY86].

### 1.3.3 Biological evolution

One of the most interesting subjects explored in statistical mechanics during the past decade is the study of the dynamics of ecosystems, that is their evolution.

In the classical Darwinian vision, which has been uncontested until the 1970s inside the scientific community, this should not represent a problem at all since the evolution is a “smooth” process. What does *smooth* mean in this context? Well, in this regard, I would like to report a passage taken from the 1859 masterpiece by Charles Darwin, “On the origin of species”:

*Natural selection is daily and hourly scrutinizing throughout the world every variation, even the slightest; rejecting all that which is bad, preserving and adding up all that is good; silently and insensibly working... We see nothing of these slow changes in progress until the hand of time has marked the long lapse of ages.*

According to this interpretation, natural selection is then “slow” and we would not be able to tell the difference in the ecosystems if we observe it during short geological times since the “hand of time” has to “mark the long lapse of ages” first. In its historic prospective, this idea is actually revolutionary. For the first time the hypothesis of a Divine creation was openly questioned on the basis of scientific findings, that is the fossils. Moreover, according to the available fossil record of that age, an almost stationary evolution was a totally acceptable hypothesis.

The situation started to get more complicated with the discovery of *mass extinctions* which characterize particular eras in time. Examples of the signatures of these sudden changes in the ecosystems are reported in Fig 1.3, borrowed from Ref. [RS82].

Paleontologists tried to find exogenous justifications for such empirical “anomalies”. The most popular scenario of an external shock leading to large scale extinction is, without any doubt, the impact of an asteroid in the Gulf of Mexico at the end of the Cretaceous period which, “traditionally”, signs the end to the reign of the dinosaurs on Earth.

A different kind of interpretation for the discontinuities in the fossil records is the one proposed by Eldredge and Gould [EG72] in the early seventies. They postulated an evolution that is almost stationary apart from periods during which it is *naturally* “punctuated” by rapid, avalanche-like, changes. This theory, referred as *punctuated equilibrium*, although being nothing more than an empirical observation in its original form, for the first time took into consideration that ecosystems can actually evolve according to a very complex, nonlinear, dynamics and not follow a “smooth” path that can be deviated just by external factors.

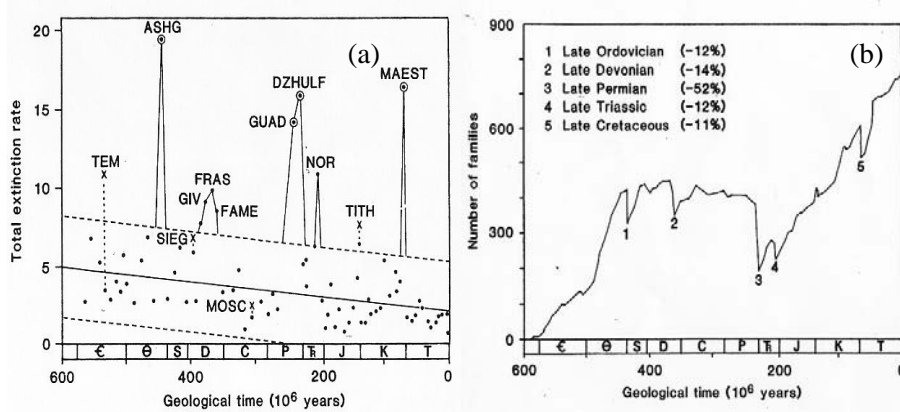


Figure 1.3: (a) Total extinction rate, measured in million years, for families of marine invertebrates and vertebrates. Statistically significant mass extinctions are evident at the end of the Ordovician (ASHG), Permian (GUAD-DZHULF), Triassic (NOR) and Cretaceous (MAEST) periods [RS82]. (b) Diversity through time for families of marine vertebrates and invertebrates. The numbers in the plot indicate five mass extinctions in which a clear drop in the biodiversity are recognizable [RS82].

This new point of view raised the attention of many physicists and put the evolutionary problem under a new light. Nowadays there is a quite general agreement in the physics community, that the dynamics of ecosystems follow a path that is actually very similar to the one observed in spin glasses. In fact, the complexity of the energy landscape at low temperatures, could represent the potential *fitness* for the ecology. If the evolving system has reached the bottom of a deep fitness valley, then we are in an almost equilibrium situation and drastic changes will rarely happen. The frequency of the changes in the ecosystem becomes inversely proportional to the barrier heights from one valley to the next. The smaller the barriers are, the more frequent the changes are. If we would check the evolution of the species in the geological record, we would find many fossils corresponding to the position at the bottom of the valley where the species remained for so long, but few or none corresponding to the crossing of the ridge, which happened very fast on the geological time scale.

Another physical interpretation of the fossil record is addressed in the framework of *self-organized criticality*. A review on the subject and the way it applies to this problem is discussed in detail in chapter 5. A general review of the statistical mechanics approach to the evolutionary problem can be found in Refs. [NP99] and [Dro01].

### 1.3.4 The stock market

In the past few years an increasing number of physicists have been involved in the study of economic systems with particular emphasis on the financial markets. Actually, this is not the first time that physics and economics have met. Newton himself, Majorana and, more recently, Mandelbrot, actively worked in this field. Nevertheless, the interest, and therefore the relative number of publications, has never been as broad as today.

What is the reason behind this sudden interest? Probably there are many, including better chances to find jobs outside the academia. But, without any doubt, a huge contribution has been given by the technological changes that took place during the '80s, leading to an electronic trading system which enabled the storage of large amounts of data. Before that period, the number of data available was quite scarce and daily data were actually considered “high-frequency”. A large sample was probably composed by something of the order of 1000 points. In these circumstances, apart from some sporadic attempts [Man97], physicists were still perplexed about studying systems which they could not empirically test against models in a statistically reliable way. But, as just mentioned, the new technologies changed everything radically: high frequency data moved from one day period to one minute in the most liquid markets and the number of samples available become easily larger of that of many physical experiments.

Once these large databases became available to the public, physicists began to tackle this new area, no more bounded by the initial skepticism. The first results were surprising: different empirical works revealed the importance of some *stylized* features of the stock market that were rarely taken into consideration by economists.

What physicists found was actually what they always suspected: the stock market is, indeed, a complex system and its dynamical behaviour is not very different from that of physical systems! This not in its loose meaning but, strictly, from a quantitative point of view. In fact concepts they were very familiar with, such as power-law distributions, correlation, scaling and random processes, appeared in the data sets. Fig. 1.4, from Ref. [MS97], shows the time series from a turbulent flow and the stock market: similarities are evident.

This new experimental revolution paved the way for applying concepts from phase transitions, statistical mechanics, nonlinear dynamics and disordered systems to the stock market that started to be regarded, *de facto*, as a physical system.

It is also important to stress that not only empirical studies were carried out but also different physically-related models started to be developed in parallel, leading to new ideas regarding the underlying basic mechanism of the stock

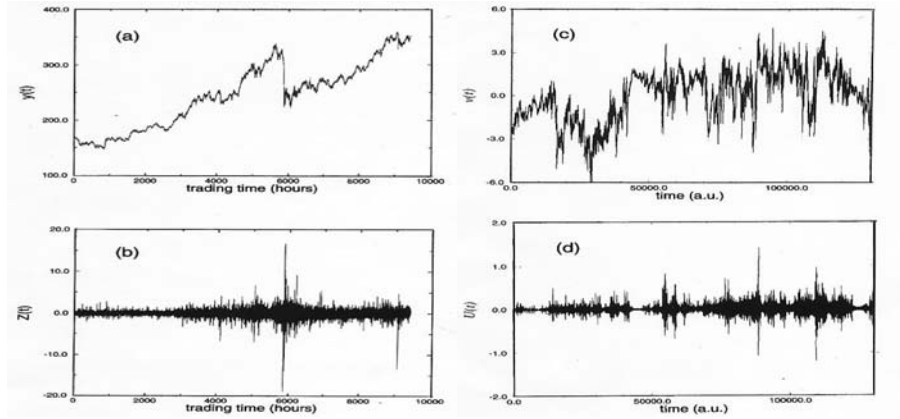


Figure 1.4: (a) S&P500 index for the US market from January 1984 to December 1989. The sampling period is 1 hour. (b) Price differences in the S&P500 calculated for the time series in (a). (c) Time series of wind velocity recorded for high Reynolds number,  $R_l \sim 1500$ , in the atmosphere. Velocity differences in the time series of plot (c). Note the similarities between these two, apparently, different systems. The plots in this figure are borrowed from Ref. [MS97].

market dynamics: well established concepts such as disordered frustrated systems, self-organization, scaling and universality were brought to this novel field of research.

Since the 1990s, papers on economic subjects started to be published in new interdisciplinary journals as well as in established ones such as *Physical Review*. At the same time conferences around the world were organized: *econophysics* was born.

Nowadays, there are a few physicists still arguing that in finance is not possible to perform large scale experiments and, therefore, it has not much to do with physics. But this claim is only partially true. Many relevant areas of physics are effected by exactly the same limitations. Examples include astrophysics, atmospheric physics and geophysics. The study of the stock market, and the economic world in general, must be considered a proper branch of complex systems research, as much as spin glasses or turbulence.

A more quantitative discussion of econophysics and its applications is left for the next chapters of the thesis. An introduction to the new emerging field can be found in the book of Mantegna and Stanley [MS99] and in the report of Feigenbaum [Fei03].

I would like to conclude this short introduction on stock markets with a mention to a fact that took place recently in an Econophysics Colloquium in

Canberra, Australia. In this occasion an economist said that if you throw a *dead bird* in the air, every physicist will be able to predict the dynamics of its body. But if the bird is *alive* there is no way the physicist can say something: this is a sociological issue. This is probably true, but this is not the way a physicist thinks either! He will never be able to predict where a *single* bird will fly but if you have a very large number of birds, hundreds of them, he will probably guess correctly what it is going to happen once you set them free (at least for a while)!

## 1.4 Outline

The rest of the thesis is organized as follows. In Chapter 2 we empirically investigate to what extent the self-organization of the stock market can be related to the physical frameworks of *self-organized criticality* and *discrete scale invariance*. In Chapter 3 we use cellular automata to show the role played by the *herding* behaviour of stochastic agents. This is linked with the large fluctuations observed in the price time series. Chapter 4 is dedicated to a numerical exploration the importance of complex, scale-free, networks both in physical and social systems. In particular, the antiferromagnetic Ising model and stochastic opinion formation are studied. The implications of explicit interactions in an extremal dynamic model for biological evolution are discussed in Chapter 5. This model can also be relevant for the dynamics of firms in the economic contest. General conclusions are left for the last chapter.





---

# Self-organization in the stock market: avalanche dynamics and log-periodic oscillations

In the present chapter we search for quantitative imprints of self-organization in one of the most widely studied complex systems: the stock market. In particular, we study the dynamics of several world-wide price indices for indications of self-organized criticality (SOC) and embedded log-periodic structures. The main feature of SOC systems is that their evolution, from one metastable state to another, takes place in avalanches of elementary events, which are triggered as soon as a certain threshold is exceeded. The criticality refers to characteristic power law distributions in size and duration of these avalanches. Self-similar, log-periodic oscillations, instead, are believed to be the result of feedback and herding processes, enhanced by a discrete scale-invariant hierarchy in market organization, during particular periods. The detection of these patterns have important implications in crash forecasting. Evidence for both phenomena are pointed out. In particular we found that the dynamics of the stock market can be described well by an avalanche behaviour alternated by quiescent periods. Correlation between the market avalanches has also been found, implying non-trivial memory effects. Moreover, we show evidence for fractal log-periodicity in the most important western indices during a recession period starting at the beginning of 2000 and lasting until the end of 2003. The results presented in this chapter are the summary of two papers published in international physical journals in 2005 [BLT05a, BDL<sup>+</sup>05].

## 2.1 Self-organization in complex systems

The term *self-organization* refers, in general, to the emergence of large-scale structures in non-linear extended systems: a macroscopic spatio-temporal ordered state emerges solely by the non-linear interactions of the microscopic elements composing the system itself. Moreover, the interactions between these elements are, most of the time, just at local level, that is, each elementary compo-

ment have no information of the global state. As for the cellular automata mentioned in the introductory chapter, short range forces are sufficient to drive the system toward a macroscopic coherent phase. The concept of pattern-emergence seems to be widely recognized in the literature as the most striking feature of self-organization. Examples of emergent natural patterns are shown in Fig. 2.1

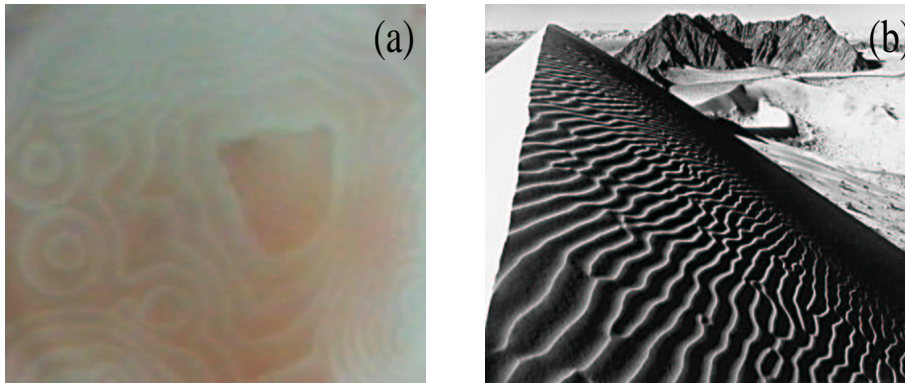


Figure 2.1: Two dimensional wave pattern in the Belousov-Zhabotinski reaction (a) and ripples in a sand dune (b).

Now, is it possible that human society itself, composed by highly individualistic people, share features of self-organization? There is no doubt that human beings have a natural tendency to modify the environment and take decisions according to their personal needs and ideas of “coherence”. This concept of “tuning” is very subjective and, in principle, there is no apparent reason why the interaction of several individuals should give rise to recurrent patterns on a large-scale.

In the present chapter we show that this is actually the case and, therefore, human society is not different from other complex systems. In particular we quantitatively study the phenomenon of self-organization in one of the most interesting and widely studied environments ruled by the human interactions: the stock market.

### 2.1.1 *Self-organization in the stock market*

Human society appears to be one of the most fascinating examples of a self-organized system. The complex interactions between individuals can give rise to patterns and coherent events similar to those observed in Nature. A widely studied example of human organization is the stock market. In this particular

case we have actual measures of the interactions between agents, that is the temporal evolution of a stock price. Under this circumstance, it is possible to quantify the strength of coherence and synchronization in human behaviour when it is driven by certain expectations, as, for example, the performance of a certain stock. Moreover, by analyzing stock market time series we can get rid of the intrinsic ambiguity associated with the term “coherent event” and “pattern” and define some proper measures for the self-organization of this system.

In sections. 2.2 and 2.3 we summarize the main concepts of a particular kind of self-organization and its relevance in the stock market context, that is the *self-organized criticality* (SOC). A possible method for revealing SOC from a time series is explained in Sec. 2.4 while the results of its application to financial data are reported in Sec. 2.5. Embedded log-periodic oscillations of the price index can be regarded as a further symptom of self-organization and correspond to an underlying *discrete scale invariance* (DSI). This subject is discussed in Sec. 2.6 and the corresponding empirical findings are shown in Sec. 2.8. Discussions and conclusions are left for the last section of this chapter.

## 2.2 Self-organized criticality: how nature works?

In the late eighties, two seminal papers by Bak, Tang and Wiesenfeld (BTW) [BTW87, BTW88], caught the attention of the physics community. In these works the authors argued that the dynamical behaviour of many complex systems can be explained by the concept of self-organized criticality (SOC) [Jen98, Tur99]. The key concept of SOC is that complex systems, although obeying different microscopic physics, may exhibit similar dynamical behaviour. In particular, the statistical properties of these systems can be described by power laws, reflecting a lack of any characteristic scale. These features are equivalent to those of physical systems during a phase transition, that is at the critical point. The applicability of this framework to natural systems has been particularly emphasized in the actual “manifesto” of self-organized criticality, the somehow controversial book of Bak “How Nature works” [Bak99].

It is worth mentioning that one of the main criticisms of this theory is that the system does not reach the critical state “naturally”, as originally claimed [BTW87, BTW88]. Rather a certain degree of implicit tuning is necessary. In particular, local conservation laws and specific boundary conditions seem to be important ingredients for the appearance of power laws [Jen98].

The classical example of a system exhibiting SOC behaviour is the 2D sand-pile model [BTW87, BTW88, Jen98, Tur99], originally proposed as a toy model for energy dissipation in turbulent flows. Here the cells of a 2D grid are ran-

domly filled, by an external driver, with “sand”. When the gradient between two adjacent cells exceeds a certain threshold a redistribution of the sand occurs, leading to more instabilities and further redistributions. The storing of energy and then a rapid dissipation in an avalanche-like fashion is probably the main feature of systems exhibiting SOC behaviour. This implies a dynamics that is governed by the presence of, at least, two well separated time scales (driver and avalanches for the sandpile) and by a threshold for discharge. The benchmark of the sandpile model, and indeed of all systems exhibiting SOC, is that the distribution of the avalanche sizes, their duration and the energy released, obey power laws.

The framework of self-organized criticality has been claimed to play an important role in solar flaring [LH91, LHMB93], space plasmas [Cea03, Vea03] and earthquakes [BT89, SS89, SDS90, HSS98] in the context of both astrophysics and geophysics. In the biological sciences, SOC, has been related, for example, with evolution/extinction of species [BS93]. Some work has also been carried out in the social sciences. In particular, traffic flow and traffic jams [NH93, Nag95, Nag85, Nag96], wars [RT98] and economics [Tur99, BCSW93, BPS97, Fei03] dynamics have been studied. A more detailed list of subjects and references related to SOC can be found in the review paper of Turcotte [Tur99].

## 2.3 Self-organized criticality and stock market dynamics

The presence of SOC in economics, seen as a complex self-interacting system have been suggested in different works [Tur99, BCSW93, BPS97, Fei03] but empirical studies are still lacking. In the present discussion we attempt to formalize the presence of SOC behaviour in the stock market in terms of scale-free avalanche dynamics. In this framework, we look at the stock market as a sort of sandpile. Periods of relative calm can be suddenly interrupted once a certain threshold, as for example the expectation of the agents, is reached and a period of frantic activity and large fluctuations of prices, equivalent to an avalanche, sets in [BLT05a].

In order to gain some insight into this problem, we analyze the tick-by-tick behaviour of the Nasdaq E-mini Futures index (NQ),  $P_r(t)$ , from 21/6/1999 to 19/6/2002 for a total of  $2^{19}$  data. A sample of this data is illustrated in Fig. 2.2(a). In particular, we study the logarithmic returns of this index, defined as

$$r(t) = \ln P_r(t) - \ln P_r(t - 1), \quad (2.1)$$

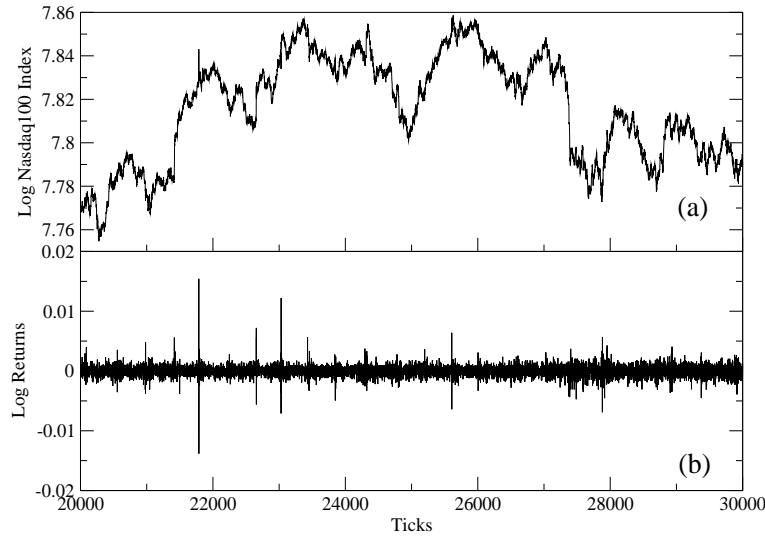


Figure 2.2: Sample of the tick-by-tick time series of the Nasdaq E-mini Futures(a), as well as the corresponding returns (b).

and plotted in Fig. 2.2(b).

To examine the extent to which our findings apply to other stock market indices we also studied the S&P ASX50 (for the Australian stock market) at intervals of 30 minutes over the period 20/1/1998 to 1/5/2002, for a total of  $2^{14}$  data points. Possible differences between daily and high frequency data have also been taken into consideration through the analysis of the Dow Jones daily closures from 2/2/1939 to 13/4/2004. The results are presented in Sec. 2.5.

From a visual analysis of the time series of returns, Fig. 2.2(b), we observe long periods of relative tranquility, characterized by small fluctuations, and periods in which the index goes through very large fluctuations, equivalent to avalanches, clustered in relatively short time intervals. These may be viewed as a consequence of a build-up process leading the system to an extremely unstable state. Once this critical point has been reached, any small fluctuation can, in principle, trigger a chain reaction, similar to an avalanche, which is needed to stabilize the system again.

The issue regarding the presence of SOC in the stock market is not only of theoretical importance, since it would lead to improvements in financial modeling, but could also enhance the predictive power [CL96] of econophysics.

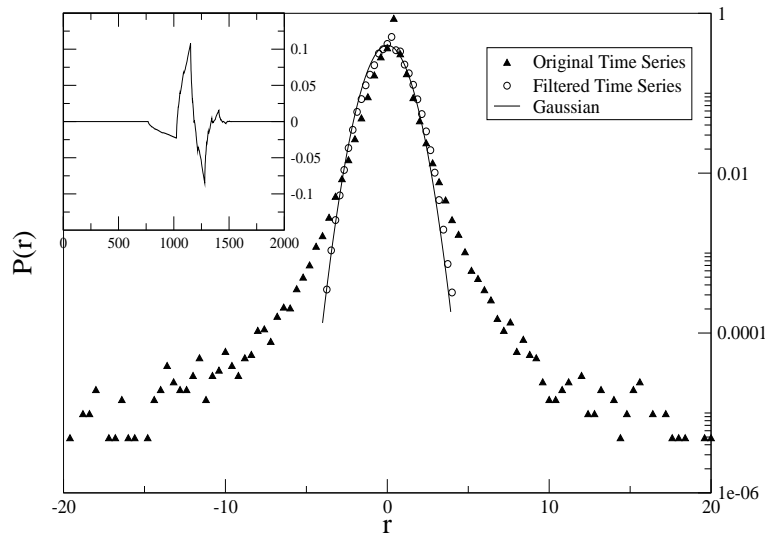


Figure 2.3: PDF of the logarithmic returns of the NQ before (triangles) and after filtering (circles), with  $C = 2$ . The original time series is reduced to the level of noise. A Gaussian distribution is plotted for comparison. The insert shows the fourth member of the Daubechies wavelets used in the filtering.

## 2.4 Looking for avalanches: the wavelet method

Recent empirical studies have shown that the dynamical behaviour of the fluctuations in financial time series is similar to that of hydrodynamic turbulence [GBP<sup>+</sup>96, MS97] – although differences have also been pointed out [MS97]. Both the spatial velocity fluctuations in turbulent flows and the stock market returns show an intermittent behaviour, characterized by broad tails in the probability distribution function (PDF),  $P$ , and a non-linear multifractal spectrum [GBP<sup>+</sup>96]. The PDF for the normalized logarithmic returns,

$$r(t) \rightarrow \frac{r(t) - \langle r(t) \rangle_l}{\sigma(r(t))}, \quad (2.2)$$

where  $\langle \dots \rangle_l$  is the average over the length of the sample,  $l$ , and  $\sigma$  the standard deviation, is plotted in Fig. 2.3. The departure from a Gaussian behaviour is evident, in particular, in the peak of the distribution and in the broad tails, which are related to extreme events.

The empirical analogies between turbulence and the stock market may suggest the existence of a temporal information cascade for the latter [GBP<sup>+</sup>96]. This is equivalent to assuming that various traders require different information

according to their specific strategies. In this way different time scales become involved in the trading process. In the present work we use a wavelet method in order to study multi-scale market dynamics.

The wavelet transform is a relatively new tool for the study of intermittent and multifractal signals [Far92]. The approach enables one to decompose the signal in terms of scale and time units and so to separate its coherent parts – that is, the bursty periods related to the tails of the PDF – from the noise-like background, thus enabling an independent study of the intermittent and the quiescent intervals [FSK99].

The continuous wavelet transform (CWT) is defined as the scalar product of the analyzed signal,  $f(t)$ , at scale  $\eta$  and time  $t$ , with a real or complex “mother wavelet”,  $\psi(t)$ :

$$W_T f(t) = \langle f, \psi_{\eta,t} \rangle = \int f(u) \bar{\psi}_{\eta,t}(u) du = \frac{1}{\sqrt{\eta}} \int f(u) \bar{\psi}\left(\frac{u-t}{\eta}\right) du. \quad (2.3)$$

The idea behind the wavelet transform is similar to that of windowed Fourier analysis and it can be shown that the scale parameter is indeed inversely proportional to the classic Fourier frequency. The main difference between the two techniques lies in the resolution in the time-frequency domain. In the Fourier analysis the resolution is scale independent, leading to aliasing of high and low frequency components that do not fall into the frequency range of the window. However in the wavelet decomposition the resolution changes according to the scale (i.e. frequency). At smaller scales the temporal resolution increases at the expense of frequency localization, while for large scales we have the opposite. For this reason the wavelet transform is considered a sort of mathematical “microscope”. While the Fourier analysis is still an appropriate method for the study of harmonic signals, where the information is equally distributed, the wavelet approach becomes fundamental when the signal is intermittent and the information localized.

The CWT of Eq.(2.3) is a powerful tool to graphically identify coherent events, but it contains a lot of redundancy in the coefficients. For a time series analysis it is often preferable to use a discrete wavelet transform (DWT). The DWT can be seen as an appropriate sub-sampling of Eq.(2.3) using dyadic scales. That is, one chooses  $\eta = 2^j$ , for  $j = 0, \dots, L-1$ , where  $L$  is the number of scales involved, and the temporal coefficients are separated by multiples of  $\eta$  for each dyadic scale,  $t = n2^j$ , with  $n$  being the index of the coefficient at the  $j$ th scale. The DWT coefficients,  $W_{j,n}$ , can then be expressed as

$$W_{j,n} = \langle f, \psi_{j,n} \rangle = 2^{-j/2} \int f(u) \psi(2^{-j}u - n) du, \quad (2.4)$$

where  $\psi_{j,n}$  is the discretely scaled and shifted version of the mother wavelet. The wavelet coefficients are a measure of the correlation between the original signal,  $f(t)$ , and the mother wavelet,  $\psi(t)$  at scale  $j$  and time  $n$ . In order to be a wavelet, the function  $\psi(t)$  must satisfy some conditions. First it has to be well localized in both real and Fourier space and second the following relation

$$C_\psi = 2\pi \int_{-\infty}^{+\infty} \frac{|\hat{\psi}(k)|^2}{k} dk < \infty, \quad (2.5)$$

must hold, where  $\hat{\psi}(k)$  is the Fourier transform of  $\psi(t)$ . The requirement expressed by Eq.(2.5) is called *admissibility* and it guarantees the existence of the inverse wavelet transform. The previous conditions are generally satisfied if the mother wavelet is an oscillatory function around zero, with a rapidly decaying envelope. Moreover, for the DWT, if the set of the mother wavelet and its translated and scaled copies form an orthonormal basis for all functions having a finite squared modulus, then the energy of the starting signal is conserved in the wavelet coefficients. This property is, of course, extremely important when analyzing physical time series [KCV01]. More comprehensive discussions on the wavelet properties and applications are given in Refs. [Dau88] and [Far92]. Among the many orthonormal bases known, in our analysis we use the fourth member of the Daubechies wavelets [Dau88], shown in the insert of Fig. 2.3. The spiky form of this wavelet insures a strong correlation for the bursty events in the time series. The following method of analysis has also been tested with other wavelets and the results are qualitatively unchanged.

The importance of the wavelet transform in the study of turbulent signals lies in the fact that the large amplitude wavelet coefficients are related to the extreme events in the tails of the PDF, while the laminar or quiescent periods are related to the ones with smaller amplitude [KCV01]. In this way it is possible to define a criterion whereby one can filter the time series of the coefficients depending on the specific needs. In our case we adopt the method used in Ref. [KCV01] and originally proposed by Katul *et al.* [Kea94]. In this method wavelet coefficients that exceed a fixed threshold are set to zero, according to

$$\tilde{W}_{j,n} = \begin{cases} W_{j,n} & \text{if } W_{j,n}^2 < C \cdot \langle W_{j,n}^2 \rangle_n, \\ 0 & \text{otherwise,} \end{cases} \quad (2.6)$$

here  $\langle \dots \rangle_n$  denotes the average over the time parameters at a certain scale and  $C$  is the threshold coefficient. Once we have filtered the wavelet coefficients  $\tilde{W}_{j,n}$  we perform an inverse wavelet transform, obtaining a *smoothed* version, Fig. 2.4(b), of the original time series, Fig. 2.4(a). The residuals of the original time series with the filtered one correspond to the bursty periods which we aim to study, Fig. 2.4(c).



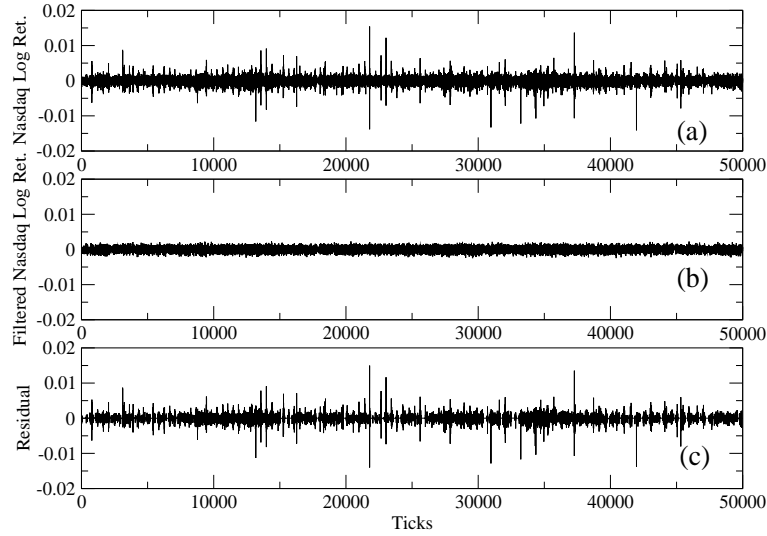


Figure 2.4: A sample of the original time series of logarithmic returns for the NQ is shown in (a), same as Fig. 2.2(b). The filtered version is shown in (b). The noise-like behaviour of this time series is evident. The residual time series is shown in (c). This corresponds to the high activity periods of the time series, related to the broad wings of the PDF. The cut-off parameter in this case is  $C = 2$ .

The time series of logarithmic prices can also be reconstructed from the residuals, as shown in Fig. 2.5. Its behaviour is very different from the one reconstructed from the filtered Gaussianly distributed returns. Note how, in the latter case, the time series is completely independent of the actual market price.

At this point one might wonder if it is possible to tune the parameter  $C$  to maximally remove the uninteresting Gaussian noise, associated with the *efficient* phase of the market where movement can be well approximated by a random walk [MS99], from the original signal. Fig. 2.6 illustrates the extent to which the filtered signal is Gaussian as a function of this parameter. Here we report the value of the excess of kurtosis,  $K_e = \langle r^4 \rangle / \langle r^2 \rangle^2 - 3$ , where  $\langle \dots \rangle$  is the average of the filtered time series over the period considered. For pure Gaussian noise this value should be 0. With this test we are able to identify  $C \sim 1$  as optimal for both the NQ and Dow Jones. The Gaussian PDF of the filtered time series,  $C = 2$ , is shown in Fig. 2.3, no skewness is present as well. Moreover, an examination of the standard autocorrelation function of the filtered time series shows a complete temporal independence, further confirming that we have successfully filtered pure Gaussian noise.

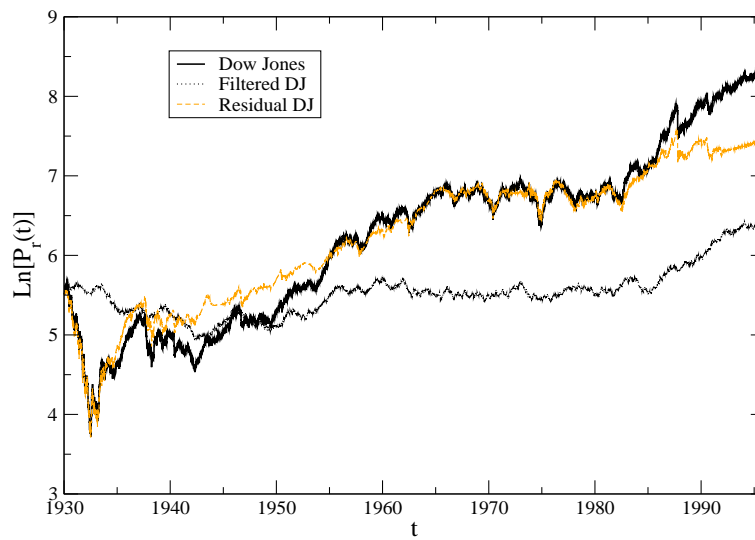


Figure 2.5: The Dow Jones time series is superimposed with the time series reconstructed from the filtered returns and the residual returns remaining after the filtered returns are subtracted from the original returns. The price behaviour generated by the “efficient” or filtered returns is largely independent of the observed price. The filtering parameter, in this case, is  $C = 1$ .

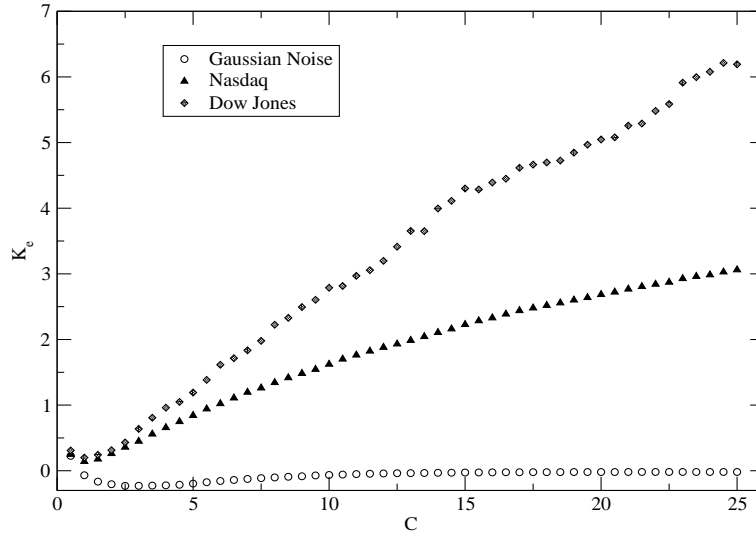


Figure 2.6: The excess of kurtosis,  $K_e$ , plotted as a function of the filter parameter  $C$  for the NQ and Dow Jones indices. A sample of Gaussian noise is also included for contrast. An optimal value of  $C \sim 1$  is found, optimally filtering the original market time series to the level of noise.

However, despite the existence of an optimal parameter for the filtering, in the next section we show that the precise value of  $C$  does not change qualitatively the results our analysis.

As a final remark, we would like to point out how a simple threshold method would not be appropriate for this kind of analysis. In fact, we would include in the filtering some non-Gaussian returns at small scales that are relevant in our analysis. This drawback is illustrated in Fig. 2.7 (Top) where the PDF for the returns of the NQ, filtered using a fixed threshold of  $r_{th} = 5$  standard deviations is shown by the open squares. In this case broad wings, related to events that do not follow Gaussian statistics, are clearly evident.

## 2.5 Empirical results

In the previous section we have introduced the wavelet method in order to distinguish periods of high activity and periods of low or noise-like activity. The results are shown in Fig. 2.3 for  $C = 2$ . Once we have isolated the noise part of the time series we are able to perform a reliable statistical analysis on the *coherent events* of the residual time series, Fig. 2.4(c). In particular, we define

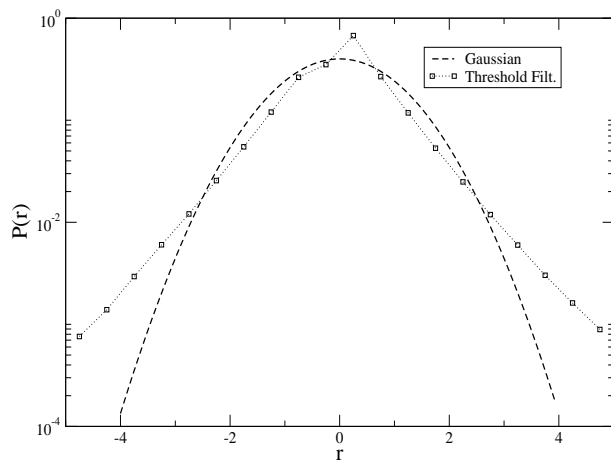


Figure 2.7: Comparison between the PDF of the original time series for the NQ and its wavelet filtered version for  $C = 1$ . A Gaussian distribution is plotted for visual comparison. The simple threshold,  $r_{th} = 5$ , method for filtering is also shown. In this case it is clear that we do not remove just Gaussian noise, but also coherent events that can be relevant for the analysis.

coherent events as the periods of the residual time series in which the volatility,

$$v(t) \equiv |r(t)|, \quad (2.7)$$

is above a small threshold,  $\epsilon \approx 0$ . The smoothing procedure is emphasized by the change in the PDFs before and after the filtering – as shown in Fig. 2.3. From this plot it is clear how the broad tails, related to the high energy events that we want to study, and the associated central peak are cut-off by the filtering procedure. The filtered time series is basically a Gaussian, related to a noise process.

A parallel between avalanches in the classical sandpile models (BTW models) exhibiting SOC [BTW87, BTW88] and the previously defined coherent events in the stock market is straightforward. In order to test the relation between the two, we make use of some properties of the BTW models. In particular, we use the fact that the avalanche size distribution and the avalanche duration are distributed according to power laws, while the laminar, or waiting times between avalanches are exponentially distributed, reflecting the lack of any temporal correlation between them [BCG<sup>+</sup>99, WSM98]. This is equivalent to stating that the triggering process has no memory.

Similar to the dissipated energy in a turbulent flow, we define the avalanche size,  $V$ , in the market context as the integrated value of the squared volatility,

over each coherent event of the residual time series. The duration,  $D_t$ , is defined as the interval of time between the beginning and the end of a coherent event, while the laminar time,  $L_t$ , is the time elapsing between the end of an event and the beginning of the next one. The time series for  $V$ ,  $D_t$  and  $L_t$  are plotted in Fig. 2.8 for  $C = 2$ .

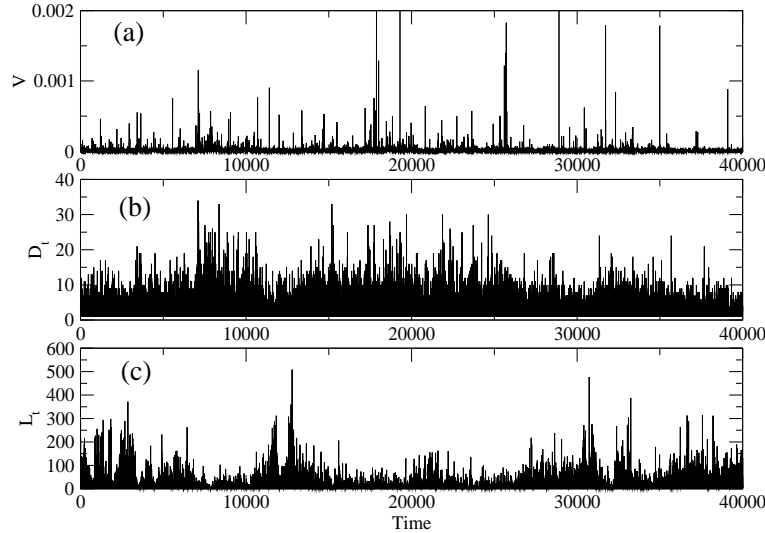


Figure 2.8: Time series for the avalanche size,  $V$ , for the NQ, (a); duration,  $D_t$ , of the avalanches, (b); and laminar times,  $L_t$  (c). The plots are obtained using  $C = 2$  as the filtering parameter.

The results for the statistical analysis for the NQ index are shown in Figs. 2.9, 2.10 and 2.11, respectively, for the avalanche size, duration and laminar times. The robustness of our method has been tested against the energy threshold, we perform the same analysis with different values of  $C$ .

A power law relation is clearly evident for all the quantities investigated, largely independent of the specific value of  $C$ . At this point is important to stress the difference in the distribution of laminar times between the BTW model and the data analyzed. As explained previously, the BTW model shows an exponential distribution for the latter, derived from a Poisson process with no memory [BCG<sup>+</sup>99, WSM98]. The power law distribution found for the stock market instead implies the existence of temporal correlations between coherent events.

This empirical result rules-out the hypothesis that the stock market is in a SOC state, at least in relation to the classical sandpile models.

In order to extend the study of the avalanche behaviour to different markets,

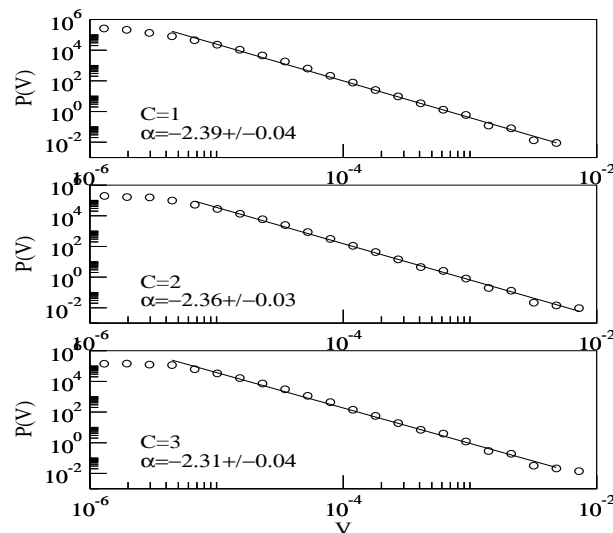


Figure 2.9: Probability distribution function for the avalanche sizes tested against several values of  $C$ . The power law behaviour is robust with respect to this parameter. Results for NQ.

we perform the same analysis over the 30 minute returns for the S&P ASX50. The results are shown in Figs. 2.12, 2.13 and 2.14. While the power law scaling for the laminar times is still very clear, the power law for the other quantities is to less precise, perhaps reflecting a different underlying dynamics compared to the NQ. On the other hand it is also important to stress the difference in length of the two time series analyzed. While for the NQ we used  $2^{19}$  data points, only  $2^{14}$  were available for the S&P ASX50, making the first study statistically more reliable.

We also investigate the possibility of differences between high frequency data and daily closures by considering a sample of  $2^{14}$  daily closures of the Dow Jones index, from 2/2/1939 to 13/4/2004. The power law behaviour is consistent with that found for the high frequency data, as shown in Figs. 2.15, 2.16 and 2.17.

Remarkably, the same power law features have been also observed in other physical contexts [BCG<sup>+</sup>99, KCV01, Sea01, Aea01, Cor04]. For the solar flaring, Boffetta *et al.* [BCG<sup>+</sup>99] have shown that the characteristic distributions found empirically are more similar to the dissipative behaviour of the shell model for turbulence [BJPV98, GC98] than to SOC. On the other hand the intermittency in turbulent flows discussed in Sec 2.4 is believed to be the result of a non-linear energy cascade that generates non-Gaussian events at small scales [Fri95] where the shape of the PDF is extremely leptokurtic. At larger scales the spatial

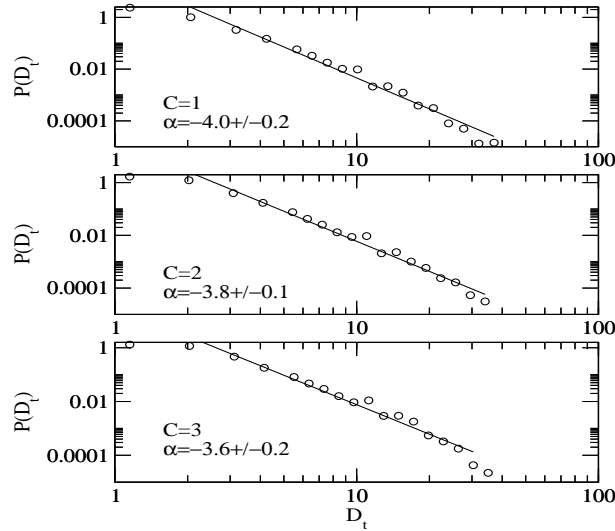


Figure 2.10: The duration of the high activity periods show a power law distribution, independent of the value of  $C$ . Results for NQ.

correlation decreases and the PDF converges toward a Gaussian. These features imply the absence of global self-similarity – which, as we have noted, is an intrinsic component of SOC models [Cea02].

Freeman *et al.* [FWR00] have argued that, although an exponential distribution holds for classical sandpile models, there exist some non-conservative modifications of the BTW models in which departures from an exponential behaviour for the  $L_t$  distribution [CO92, OC92, HK92, CC92] are observed in the presence of scale-free dynamics for other relevant parameters. The question remains whether or not these systems are still in a SOC state [FWR00]. If we assume that the power law scaling of the laminar times corresponds to a breakdown of self-organized criticality, then we face the problem of how to explain the observed scale-free behaviour of the non-conservative models. This ambiguity can be resolved if we assume that the system is in a *near-SOC* state, that is the scaling properties of the system are kept even if it is not exactly critical and temporal correlations may be present [FWR00, CP00]. Another possible scenario is related with the existence of temporal correlations in the driver [DLRVV97, NCML01, SNC02, LdAG05, BM05]. In this case the power law behavior of the waiting time distribution would be explained and the realization of a SOC state preserved [DLRVV97, SNC02].

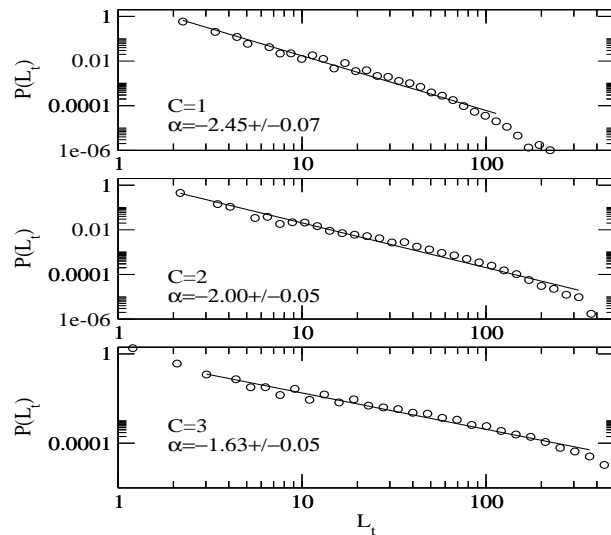


Figure 2.11: Power law distribution of laminar times for different values of  $C$ . Results for NQ.

## 2.6 Self-similar log-periodic oscillations in the stock market: self-organization and predictability

We have seen that, in the context of self-organized criticality, complex systems can evolve according to an intermittent, avalanche-like dynamics. In this fractal framework, the very large events are nothing but a magnification of the smaller ones and, therefore, present no peculiarity. This fact, in a certain way, makes predictions in the SOC environment very difficult, as a proper formalism in this direction is still lacking, although there have been some attempts [CL96].

On the other side, it is well known that extreme events, or *outliers*, can rise in periods of high activity. These can be regarded as self-generated *shocks* that may influence the dynamics of the systems for a relative long periods after their appearance. Examples of this behaviour in complex systems include earthquakes, landslides and volcanic eruptions [Sor98]. The stock market itself is not an exception. During stock market crashes, as for example the one of October 1987, millions and millions of dollars evaporate in few minutes. Because of their peculiar nature, we may think about using a specific framework, possibly fractal and related to self-organization, in order to have insight into the dynamics. As it



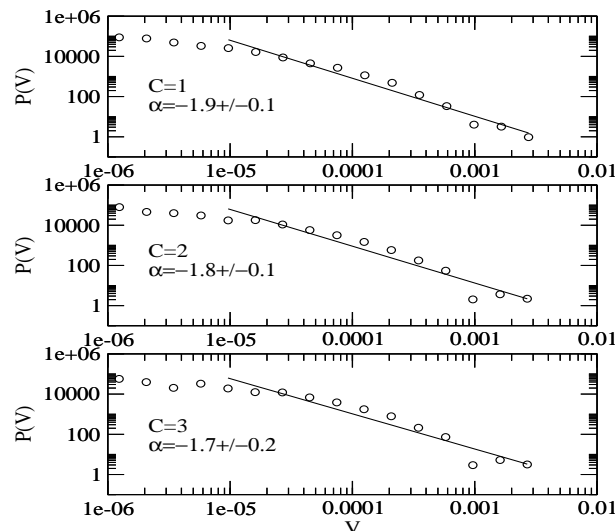


Figure 2.12: Probability distribution function for the avalanche sizes for the S&P ASX50, from 20/1/1988 to 1/5/2002.

is possible to imagine, finding a proper theory for the description of these events would be of great practical and theoretical importance since it would deeply enhance the chances of anticipating, and therefore preventing, risky situations.

Some authors [Sor03b] have attributed the market crashes to a slow build-up of long range correlations between agents operating in the market itself, leading to a self-reinforcing imitating, or “herding”, behaviour. Once the system has reached the critical state it becomes so sensitive that every exogenous shock, that is every small perturbation, can lead to a collapse: a large part of the agents involved in the trading can synchronize to sell their stocks.

On the other side, what has been empirically observed is that the build-up process leading to the crash is characterized by a power law increase of the price with superimposed log-periodic oscillations. The same kind of patterns have also been observed in recovery periods after market crashes [Sor03b, Sor03a]. The presence of these log-periodic structures before and after stock market crashes can be interpreted as an imprint of an intrinsic *discrete scale invariance* (DSI) in this complex system [Sor03b].

In the next section we give a brief introduction of the DSI framework. Moreover, to shed some light on this debated issue, we analyze the daily closures of four of the most important indices worldwide since 2000: the DAX for Germany and the Nasdaq100, the S&P500 and the Dow Jones for the United States. The results are presented in Sec. 2.8. In the same section we also show the spec-

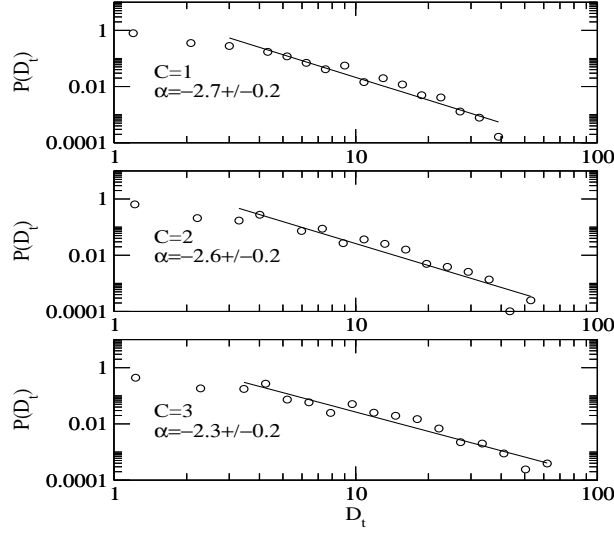


Figure 2.13: Distribution of the duration of the *coherent events* for the S&P ASX50.

tral similarities between the data and the Weierstrass-type function, used as a prototype of a log-periodic fractal function.

## 2.7 Discrete scale invariance

It is well known that many physical systems undergo phase transitions around specific critical points in the parameter space [Sta71, Sor04]. Near these points the system is strongly correlated and many characteristic quantities can be approximated well by power laws, related to the scale-invariance of the system in that state. If we assume that  $\phi(t)$  is an observable near a critical point,  $t_c$ , as for example the susceptibility of the Ising model near the critical temperature, for a change of scale  $t \rightarrow \lambda t$  we have

$$\phi(\lambda t) = \mu \phi(t), \quad (2.8)$$

where  $\mu = \lambda^\alpha$  since  $\phi(t) \sim t^\alpha$ . The power law is a solution of Eq.(2.8) for  $\forall \lambda$ .

A weaker version of the over mentioned scale invariance is the *discrete-scale invariance* (DSI) [Sor98]. In this case the system becomes self-similar only for an infinite but countable set of values of the parameter  $\lambda$ . That is Eq.(2.8) holds only for  $\lambda = \lambda_1, \lambda_2, \dots$  where in general  $\lambda_n = \lambda^n$ . In this case  $\lambda$  represents a preferential scaling factor that characterizes a hierarchical structure in the

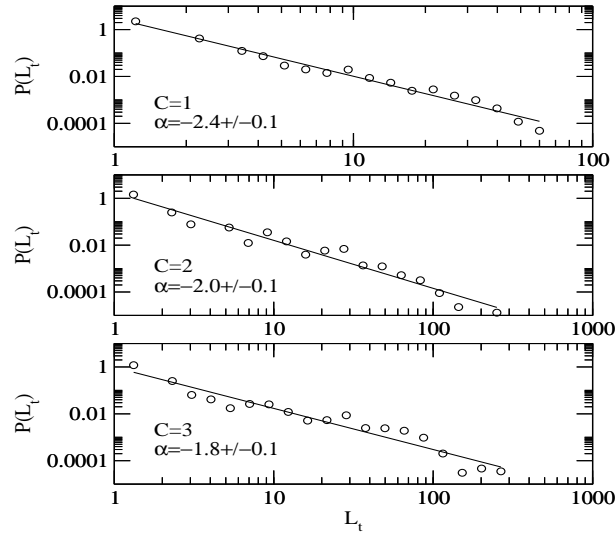


Figure 2.14: Distribution of laminar times for S&P ASX50 index.

system. The solution of Eq.(2.8) can be written in a more generic form that accounts also for a possible discrete scale invariance:

$$\phi(t) = t^\alpha \Theta \left( \frac{\ln(t)}{\ln(\lambda)} \right), \quad (2.9)$$

where  $\Theta$  is an arbitrary periodic function of period 1. Using a first order Fourier expansion on Eq.(2.9) and writing  $t \rightarrow |t_c - t|$  we obtain

$$\phi(t) = A_1 + A_2 |t_c - t|^\alpha + A_3 |t_c - t|^\alpha \cos(\omega \ln |t_c - t| - \varphi), \quad (2.10)$$

where  $\omega = 2\pi/\ln(\lambda)$ . The dominant power law behaviour, a hallmark of all critical phenomena, and the log-periodic corrections to the leading term are the main features of Eq. (2.10).

Sornette, Johansen and Bouchaud [SJB96, SJ97] first pointed out how different price indices in the stock market show a power law increase with superimposed accelerating oscillations just before a crash. The remarkable fact was that the log-periodic formula (2.10), derived for DSI systems, provided a very good approximation for this empirical fact. This led them to conjecture about the existence of a critical point in time,  $t_c$ , for which the market can undergo a phase transition (crash).

According to this framework the stock market is seen as a self-organized system that drives itself toward a critical point. Just as the Ising model has a parameter governing the temperature of the system and a critical temperature

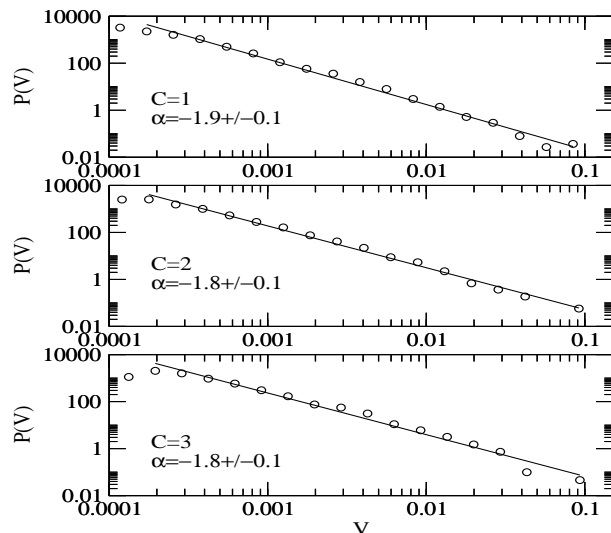


Figure 2.15: Probability distribution function for the avalanche sizes for the Dow Jones daily closures, from 2/2/1939 to 13/4/2004.

where the system undergoes a phase transition, it is postulated that the market also has such an underlying parameter which takes the critical value at time  $t_c$ . The appearance of log-periodic oscillations has been related to a *discrete* hierarchal structure of the traders. Near the critical point, when the market is very compact and unstable, every perturbation can spread throughout the system: a common decision to sell by a certain group in the hierarchy of traders can trigger a *herd* effect, leading to a crash. This concept, in a way, is similar to SOC.

Since the first paper by Sornette, Johansen and Bouchaud [SJB96] many physicists have been attracted by the idea of phase-transitions in a self-organized stock market [FF96, VBMA98, DRS99, DGRS03], even if criticisms have been also raised [LPC<sup>+</sup>99, Ili99, Fei01]. A recent review on the subject can be found in Ref. [Sor03b].

An intriguing scenario has been proposed by Drożdż and coworkers [DRS99, DGRS03]. Inspired by theoretical consistency arguments, they found empirical evidence that short time log-periodic structures can be nested within log-periodic structures on a larger scale. The appearance of these self-similar periods, one inside the other, has been related to the underlying fractal nature of the DSI, giving rise to a multi-scale log-periodicity. Moreover, the existence of a preferential scaling ratio  $\lambda \sim 2$  has been pointed out for both the leading pattern and the related sub-structures. This last fact led them to formulate a univer-

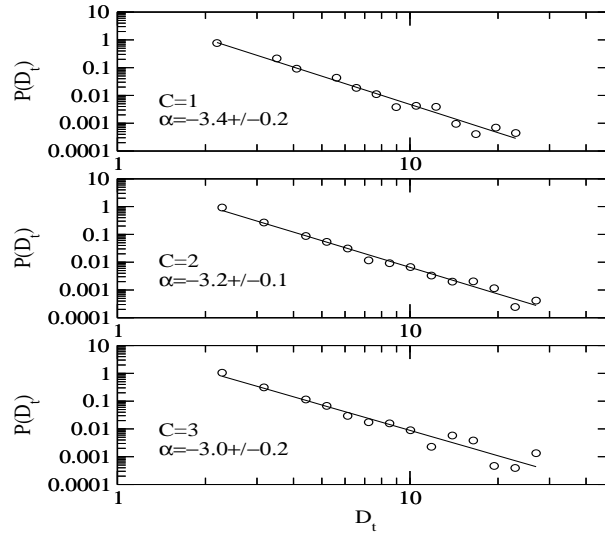


Figure 2.16: Distribution of the duration of the Dow Jones index.

sality hypothesis for the parameter  $\lambda$  and as a consequence they fixed *a priori* the frequency of the oscillations to correspond to  $\lambda = 2$ . In this way, the predictive power of Eq. (2.10) increases considerably [DRS99, DGRS03]. Further evidence of embedded sub-structures has been reported recently by Sornette and Zhou [SZ03, ZS04].

Log-periodic patterns have been observed not only in bullish periods of the market but also during the “antibubbles”, or bearish periods, that follow a market peak [JSL99, SZ02, DGRS03, ZS03a]. An example of these log-periodic oscillations has been documented during the long period of recession experienced by most of the world stock markets since the middle of 2000 [ZS03a]. In this period, which ends approximately (in our understanding) in the first months of 2003, all the most important markets world-wide are remarkably synchronized. A simple plot of the logarithmic indices,  $P_r(t)$ , is provided Fig. 2.18. We believe this is sufficient to convince the reader of this behaviour. It is nothing but an expression of the growing globalization of the modern economy [DGRS01].

In the present work we focus on the study of the daily closures of three of the most important international indices from 2000 until the end of September 2004: the DAX for the German market and the S&P500, the NQ and the Dow Jones<sup>4</sup> for the American market. We confirm (within our DSI model of Eq. (2.9)),

<sup>4</sup>The Dow Jones index has been included for historical, more that economic, reasons. In fact, it constitutes just a small sub-set of the S&P500 basket but, nevertheless, it is considered by many to be a good indicator for the health of the economy.

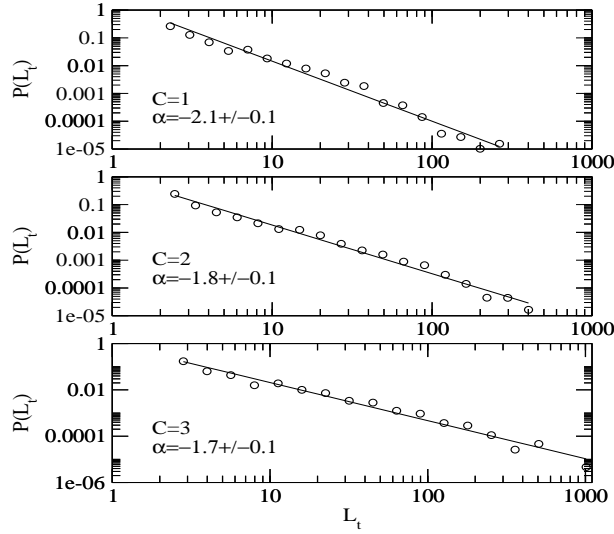


Figure 2.17: Distribution of laminar times for the Dow Jones index.

the existence of a main log-periodic structure starting in September 2000 and ending in November 2002 for all the indices in Sec. 2.8. Moreover, for the first time, we identify a clear bearish sub-structure, starting around the 15th of May 2002 and ending one year later. Ongoing log-periodic oscillations with the same characteristic frequency, starting in January 2004, also are reported.

We also address the question of a possible universality of the power law exponent  $\alpha$ , related to the trend of the time series. We then convert the S&P500, Nasdaq100 and the Dow Jones in Euros while the DAX is expressed in American Dollars. The conversion, while leaving the oscillations unaltered, seriously distorts the trends. Therefore, no universal characteristic can be claimed for this parameter.

A Lomb analysis of the main structure and the relative sub-structure, presented in Sec. 2.8.1, reveals that the dominating frequency of both is related to a common value of  $\lambda$  that is  $\lambda \sim 2$ . A second relevant harmonic, at a frequency double that of the fundamental, is also present. These results confirm the fractal hypothesis of Drożdż *at al.* [DRS99, DGRS03]. Further indications pointing to self-similar log-periodicity have been found using a Lomb analysis of a Weierstrass-type function [BL80, GS02], taken as prototype of a log-periodic fractal function. The relevance of such a function for stock market log-periodic criticality was suggested for the first time in Ref. [DRS99].

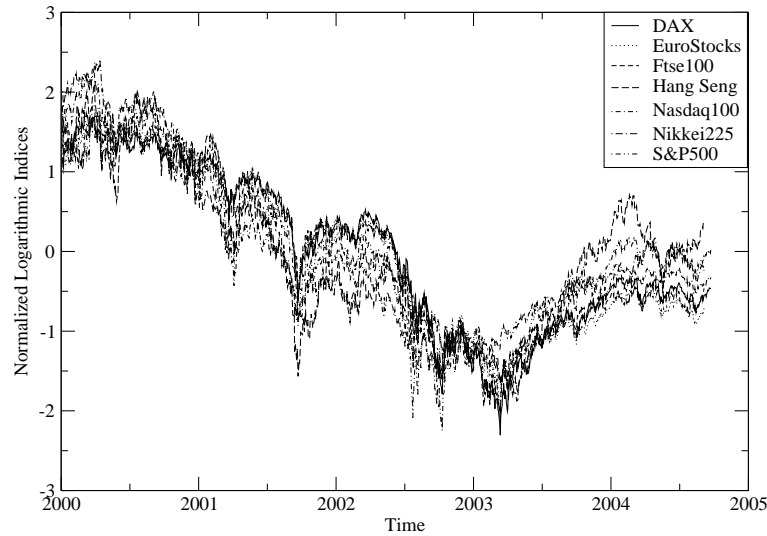


Figure 2.18: Time series of the logarithm of the most important indices worldwide since 2000. The time series have been appropriately normalized,  $P_r(t) \rightarrow \frac{P_r(t) - \langle P_r(t) \rangle}{\sigma(P_r(t))}$ , where  $\langle \dots \rangle$  denotes the average over the period under consideration and  $\sigma$  is the standard deviation. The synchronization of the indices during the recession period, and further on for some, is an expression of the modern globalized economy. The year tick in the graph marks the position of the 1st of January of the year itself.

## 2.8 Evidence of embedded log-periodic oscillations in western stock markets from 2000

The DSI model of Eq. (2.10) is used to fit the logarithm of the DAX, Nasdaq100, S&P500 and Dow Jones. Considering that the periodic function  $\Theta$  is arbitrary, we take the modulus of the cosine as it provides a better representation of the data [DGRS03] than the cosine itself. The fitting procedure that we use is borrowed from Ref. [SJB96]. According to that we express the parameters from  $A_1$ ,  $A_2$  and  $A_3$  of Eq. (2.10) as a function of  $\alpha$ ,  $\omega$  (or  $\lambda$ ),  $\varphi$  and  $t_c$  by imposing the constraint that the cost function,  $\chi^2$ , has a null derivative with respect to them. Following the method by Drożdż *at al.* [DRS99, DGRS03], we fix the parameter  $\lambda$ , considering it to be a universal constant. In particular we choose  $\lambda = 2$ . If this assumption turns out to be confirmed, then the predictive power

of the model will be increased considerably. Moreover, as we are interested here in bearish periods only and not in predicting the most probable crash time, we introduce a further simplification by adjusting  $t_c$  visually. In this way there are only two parameters left to explore:  $\alpha$  and  $\varphi$ . The results of the fits are shown in Figs. 2.19, 2.20, 2.21 and 2.22 for the DAX, the Nasdaq100, the S&P500 and Dow Jones respectively.

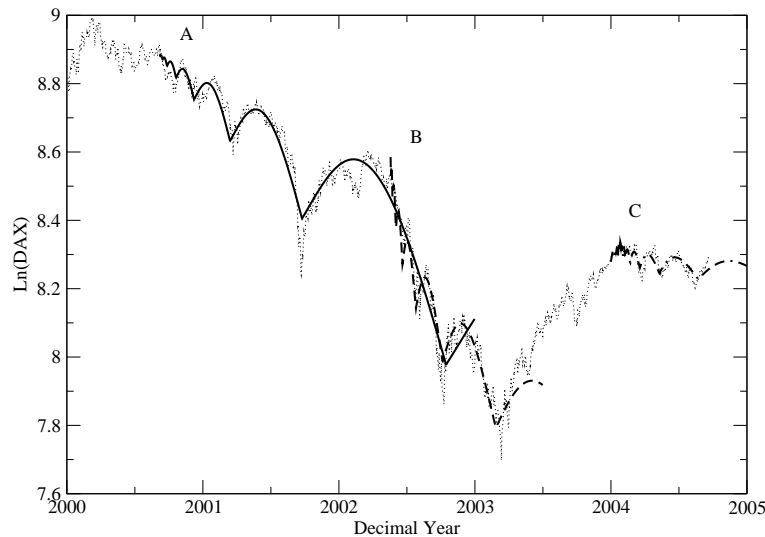


Figure 2.19: Time series of the DAX from 1/1/2000 until 22/9/2004. A log-periodic structure of the approximate duration of two years and starting in September 2000 is highlighted by the solid curve labeled (A). In this case we fix  $t_c = 1/9/2000$  in Eq. (2.10). A one year sub-structure is visible starting in May 2002, as illustrated by the dashed curve (B) ( $t_c = 16/5/2002$ ). The dashed dotted curve labeled (C) ( $t_c = 26/1/2004$ ) is related to the ongoing log-periodic oscillations. For all the fits we fixed  $\lambda = 2$ .

A log-periodic structure starting around the 1st of September 2000 and finishing in November 2002 is clearly evident for all the sets of data considered. Moreover a nested sub-structure starting around the 15th of May 2002 is also visible. Log-periodic oscillations also characterize the present state of the market. A possible origin of this behaviour can be localized at the end of January 2004.

At this point it is important to emphasize that the previous fits are obtained for a preferential scaling coefficient,  $\lambda = 2$ . This is already a good indication of the universal nature of the hierarchical scaling in stock markets.

Another interesting point regards the universality of the parameter  $\alpha$ , related



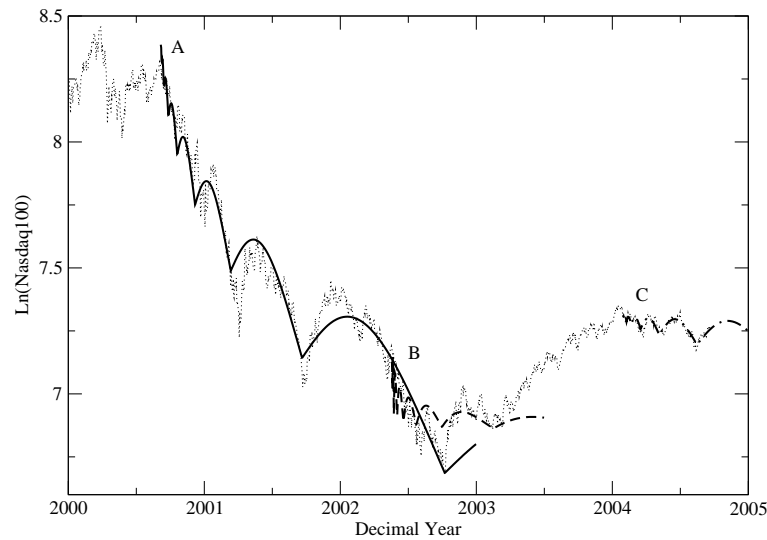


Figure 2.20: Time series for the Nasdaq100 index from 1/1/2000 until 22/9/2004. The critical times and the coding are the same as in Fig. 2.19. The sub-structure starting in May 2002 is not as evident as for the S&P500 or DAX.

to the main trend of the time series. In order to have some insight into this direction we repeat the previous fits after the conversion of the various indices into different currencies. That is we transform the DAX from Euros to American dollars, and the Nasdaq100, S&P500 and Dow Jones from American dollars to Euros. The results are shown in Figs. 2.23, 2.24, 2.25 and 2.26.

It appears clear from the plots that, while the oscillatory structures are unaltered by the currency conversion, the trends experience a serious distortion and therefore we cannot extract a universal characteristic for the exponent  $\alpha$ . On the other hand, one might wonder to what extent the market dynamics are digested in a currency other than the native currency<sup>3</sup>.

### 2.8.1 A non-parametric approach: the Lomb analysis

In order to justify our assumption of  $\lambda = 2$  we perform a non-parametric test on the angular frequency value of the log-periodic oscillations. Following the method proposed by Johansen *et al.* in Ref. [JSL99], we analyze the time series

<sup>3</sup>The problem of a change in the currency of the S&P500 index has been addressed also in Ref. [ZS05]. In this case it was argued that the main source of distortion of this index is related to the depreciation of the American dollar due to the feedback action of the Federal Reserve Bank.

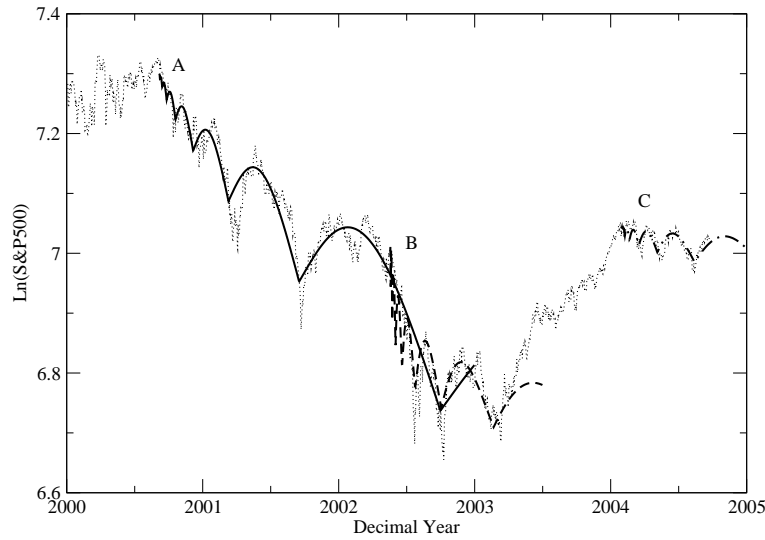


Figure 2.21: Time series for the S&P500 index from 1/1/2000 until 22/9/2004. The critical times and coding are the same as in Fig. 2.19.

of residuals,  $R(t)$ , obtained by removing the leading power law trend in the logarithm of the price,  $P_r(t)$ , according to

$$R(t) = \frac{P_r(t) - A_1 - A_2|t_c - t|^\alpha}{A_3|t_c - t|^\alpha}. \quad (2.11)$$

If the model of Eq. (2.10) reproduces the behaviour of the market correctly then the residual dependence on in the variable  $\ln(|t_c - t|)$  must be a cosine function and a spectral analysis should reveal a high peak corresponding to the angular frequency  $\omega$ .

Once we have obtained the residuals, shown in the inserts of Figs. 2.27, 2.28 and 2.29, we apply a spectral decomposition of these signals according to the Lomb algorithm [PTVF94]. This spectral algorithm makes use of a series of local fits using a cosine function with a phase and provides some practical advantages, compared to the classical Fourier transform, when the data under examination are not evenly sampled, as in our case. The results of the Lomb analysis for the periods under consideration are presented in Figs. 2.27, 2.28 and 2.29. In these plots the angular frequency corresponding to  $\lambda = 2$ , that is  $\omega \approx 9.06$ , is represented by a vertical dashed line. The results of the analysis show, for all the periods, a dominating peak in the vicinity of  $\lambda = 2$ . This fact brings more evidence to the existence of a universal scaling factor  $\lambda \approx 2$ . It is also important to underline how the Lomb analysis shows, in most of the cases, a second main frequency that is about two times the leading frequency.

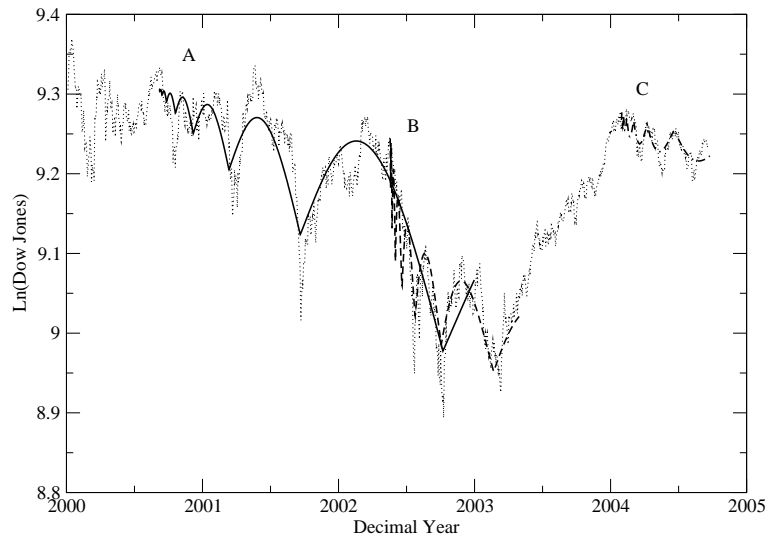


Figure 2.22: Time series for the Dow Jones index from 1/1/2000 until 22/9/2004. The critical times and coding are the same as in Fig. 2.19.

We can also assign a confidence level to the main peaks found in the analysis. Following the technique proposed in Ref. [ZS02], the ratio between the two highest peaks in the Lomb periodogram is used to give an estimation of the significance level of the higher peak. In selecting the peaks for the ratio are excluded the higher-order harmonics, multiples of the fundamental. All the ratios found from our analysis are clustered in a range approximately between 3 and 6, except for the Nasdaq100 index of Fig. 2.28. Even for a ratio of about 3, the confidence level is higher than 99% assuming Gaussian noise [ZS02]. If, instead, we assume that the noise is temporally correlated, then a fractional Brownian motion [Fed88] with Hurst exponent,  $H$ , at the worst, unrealistic, case of  $H = 0.9$ , provides a confidence level which remains greater than 80% [ZS02]. Hence all the peaks found by the Lomb analysis show a high statistical significance, with the only exception being that of the Nasdaq100 where the first peak has a low confidence level.

In order to have a better understanding of the spectral patterns just found, we test the same method of analysis on a Weierstrass-type function [BL80, GS02]. The Weierstrass-type functions are a particular solution of the discrete renormalization group equation for critical phenomena [Sor04, GS02]. Defined in the interval  $[0,1]$ , these functions are characterized by a self-similar hierarchy of log-periodic structures accumulating at a critical point  $t_c$  ( $t_c$  can be 0 or 1 according to particular choices of the parameters). Zhou and Sornette have shown that

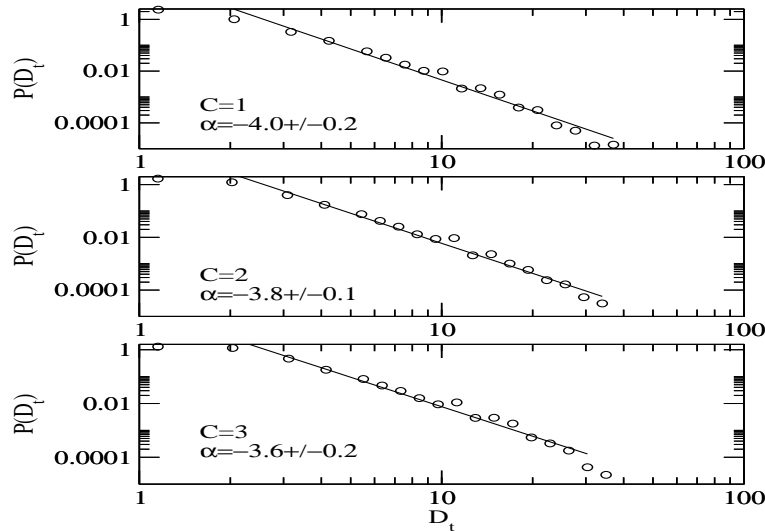


Figure 2.23: The DAX expressed in American dollars. Features are as described in Fig. 2.19.

Weierstrass-type functions can provide a good approximation for the bearish period of the stock market starting from 2000 [ZS03b].

The following Weierstrass-type function [Sor04,GS02] has been used as a test for the Lomb method:

$$f_W(t) = \sum_{n=0}^{\infty} \frac{1}{\lambda^{(2-D)n}} \exp[-\lambda^n t \cos(\gamma)] \cos[\lambda^n t \sin(\gamma)], \quad (2.12)$$

where  $\gamma \in [0, \pi/2]$  is a parameter that fixes the oscillatory structures. If  $\gamma = \pi/2$  then the parameter  $D$  corresponds to the fractal dimension of the function. For  $\gamma < \pi/2$  the function becomes smooth and it is no longer fractal [Sor04,GS02] but preserves the large scale log-periodic oscillation. Characteristic curves are illustrated in Fig. 2.30.

Once we have chosen the test function, the same procedures as used for the stock market time series are applied to the artificial time series generated by Eq. (2.12) with  $\lambda = 2$  fixed. In this case the Lomb analysis reveals for the fractal case ( $\gamma = \pi/2$ ), apart from the clear peak at the main frequency, other smaller, high frequency harmonics regularly spaced, as illustrated in Fig. 2.31.

The higher frequency periodic peaks are a manifestation of the fractality of the function itself. In fact, for  $\gamma < 1$  those frequencies are absent. The high frequency harmonics, in the pure fractal case ( $\gamma = \pi/2$ ), are a reflection of the self-similarity of the function at different scales.

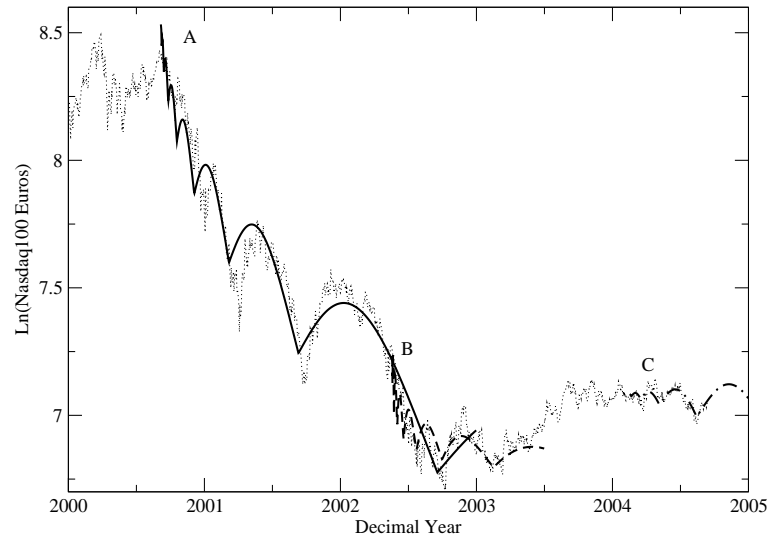


Figure 2.24: The Nasdaq100 expressed in Euros. Features are as described in Fig. 2.19.

Remarkably, the real data has similar high frequency modes that have about the same spacing as the ones artificially obtained with the Weierstrass-type function. We can also conjecture that these modes are related, as in the previous case, to self-similar structures in the time series. Of course, because of the lack of points and noise effects, these harmonics are not as clear as for the Weierstrass-type function.

The similarity in the spectral pattern between real and artificial data is an indication of the existence of self-similar structures at different scales in stock market time series, providing further support for the fractal framework of Drożdż and coworkers [DRS99, DGRS03]. The sub-structure starting in May 2002 is a clear example of self-similarity in stock market dynamics.

## 2.9 Discussion and conclusion

In the present chapter we have presented empirical evidence of self-organization in the stock market. In particular, we looked for the distribution of high activity periods, or avalanches, and self-similar log-periodic oscillation.

In the first study we have quantified the relevance of self-organized criticality in financial trading. A proof that SOC plays a central role would be of great

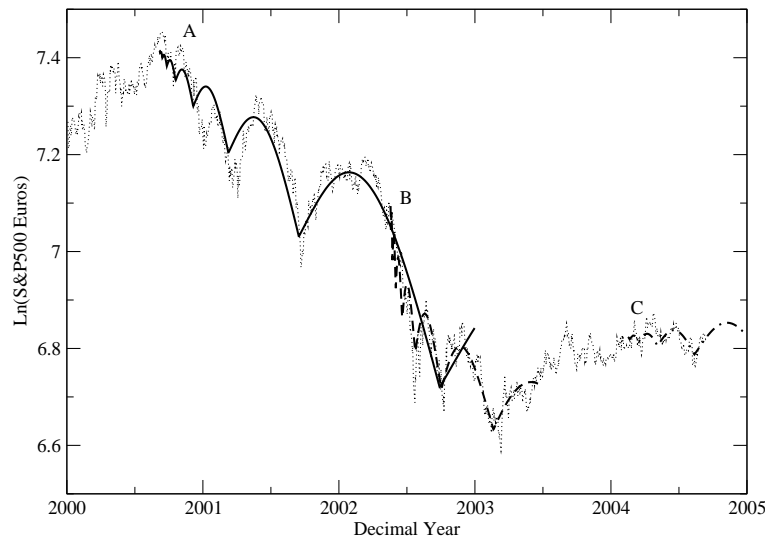


Figure 2.25: The S&P500 converted from American dollars to Euros. Features are as described in Fig. 2.19.

theoretical importance, as this would impose some constraints on the dynamics of this complex system. In fact, a bounded attractor in the state space would be implied. Moreover, it would be possible to build new predictive schemes based on this framework [CL96].

From the wavelet analysis on a sample of high frequency data for the Nasdaq E-mini Futures index, we have found that the behaviour of high activity periods, or avalanches, is characterized by power laws in the size, duration and laminar times. The power laws in the avalanche size and duration are a characteristic feature of a critical underlying dynamics in the system, but this is not enough to claim the self-organized critical state. In fact the power law behavior in the laminar time distribution implies a memory process in the triggering driver that is absent in the classical BTW models, where an exponential behavior is expected. These findings extend beyond the Nasdaq E-mini Futures index analysis: similar quantitative behaviour has been observed in the S&P ASX50 high frequency data for the Australian market and the daily closures of the Dow Jones index for the American market. The exponents found for the power laws are not universal across the indices. This would be expected in the case of a near-SOC dynamics where the shape of the distribution can be influenced by the degree of dissipation of the system which is likely to change from market to market.

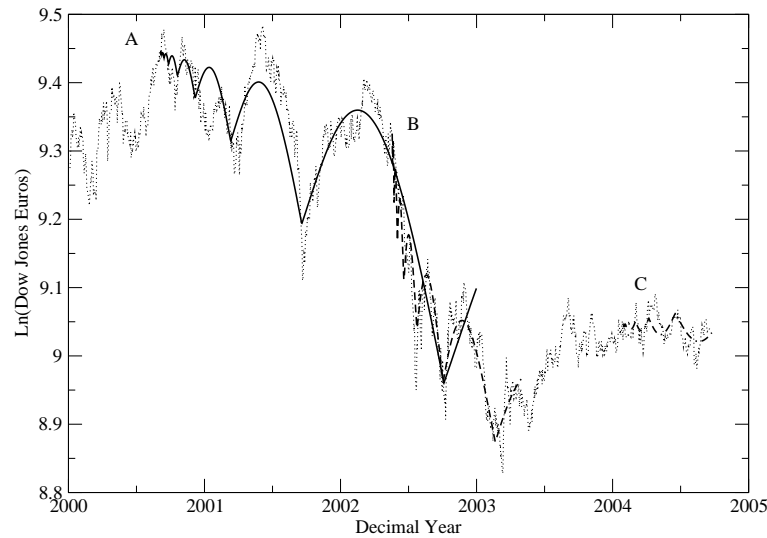


Figure 2.26: The Dow Jones converted from American dollars to Euros. Features are as described in Fig. 2.19.

Therefore, we can say that, a definitive relation between SOC theory and the stock market has not been found. Rather, we have shown that a memory process is related with periods of high activity. This does not rule out completely the hypothesis of underlying self-organized critical dynamics in the market. Non-conservative systems near the SOC state can still show power law dynamics even in presence of temporal correlations of the avalanches [FWR00, CP00]. Another possible explanation is that the memory process, possibly chaotic, is intrinsic in the driver. In this case the power law behavior of the waiting time distribution would be explained and the realization of a SOC state preserved [DLRVV97, SNC02].

The investigation of DSI has led to the identification of, at least, three clear log-periodic periods which characterize the behaviour of some of the most important indices worldwide since the year 2000. Moreover, one of the log-periodic structures found is embedded in a longer one, interestingly, both in the decelerating market phase. This finding supports the hypothesis of self-similar log-periodicity proposed by Drożdż and coworkers [DRS99, DGRS03]. A non parametric analysis over these periods has also been performed. The results of the analysis confirm the existence of log-periodic structures. Moreover, we found further evidence for a preferential scaling factor of  $\lambda \sim 2$ . The presence of a higher order harmonic at a frequency that is double the fundamental can also be related to the fractal structure of the time series. A test on a Weierstrass-

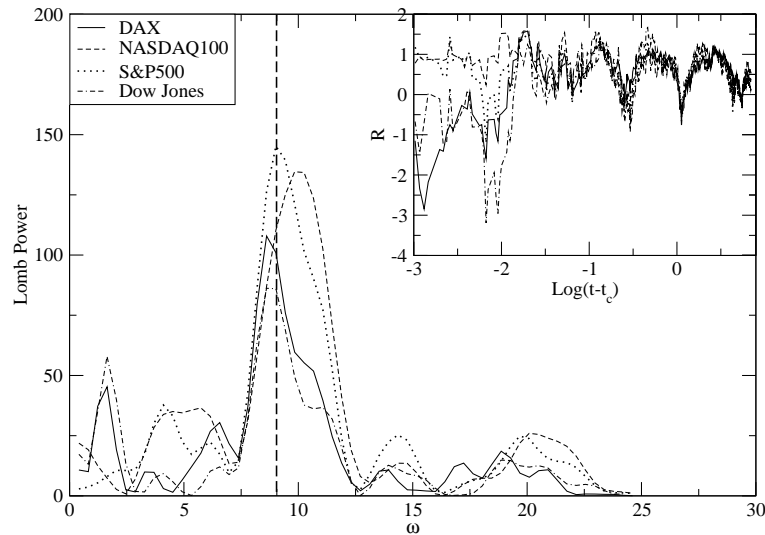


Figure 2.27: Lomb analysis for the DAX (solid line), Nasdaq100 (dashed line), S&P500 (dotted line) and Dow Jones (dashed-dotted line) during the period from 1/9/2000 to 30/12/2002. A main frequency around  $\tilde{\omega} = 9.06$  ( $\lambda = 2$ ), dashed vertical line, is clearly evident. Another important harmonic contribution can be seen at  $\omega \approx 2\tilde{\omega}$ . In the insert the residuals, with the same coding, are plotted.

type function supports this hypothesis. We have also investigated a possible universality of the power law index  $\alpha$ . For this purpose we have converted the price time series to different currencies, namely the DAX from Euros to American Dollars and the Nasdaq100, the S&P500 and the Dow Jones from American dollars to Euros. While the log-periodic oscillations remain unaltered by this procedure, the trends come to be seriously distorted and no universality can be claimed.

In conclusion, we found clear evidence of self-organization in the stock price and its logarithmic returns. The relevance of a memory process has also been pointed out for both of them. In particular, the temporal correlation of high activity periods in the returns can be the result of some kind of dissipation of information, similar to turbulence, or a memory process intrinsic in the driver itself. Of course, a combination of the two processes can also be possible. The non-linear reaction of a discrete hierarchical organization to positive or negative feedback from the market itself can play a fundamental role in the appearance of embedded log-periodic oscillations in the price indices.

Further theoretical and numerical studies are necessary to properly understand these phenomena and, possibly, to find a coherent link between the two



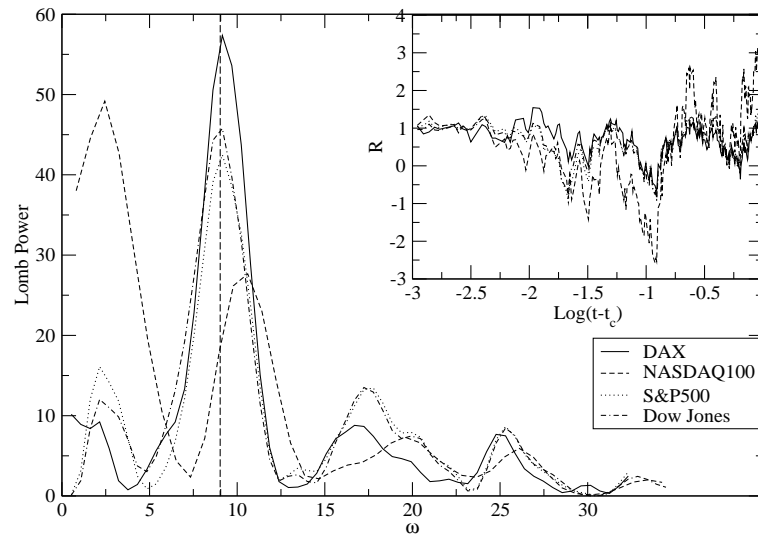


Figure 2.28: Lomb analysis for the DAX (solid line), Nasdaq100 (dashed line), S&P500 (dotted line) and Dow Jones (dashed-dotted line) during the period from 16/5/2002 to 3/5/2003. Regular high order harmonics are still present. As already seen from the fit, the log-periodic behaviour of the Nasdaq100 index is not as clear as for the other indices. The residuals are presented in the insert.

of them.

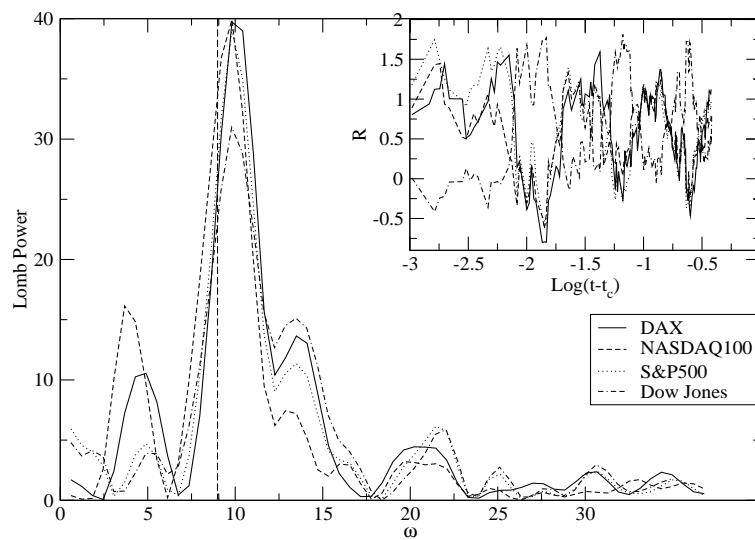


Figure 2.29: Lomb analysis for the DAX (solid line), Nasdaq100 (dashed line), S&P500 (dotted line) and Dow Jones (dashed-dotted line) during the period from 26/1/2004 to 22/9/2004. A main frequency along with other higher order harmonics are revealed. In this case the phase of the residuals for the Dow Jones differs from the other indices, reflecting a less than perfect synchronization.

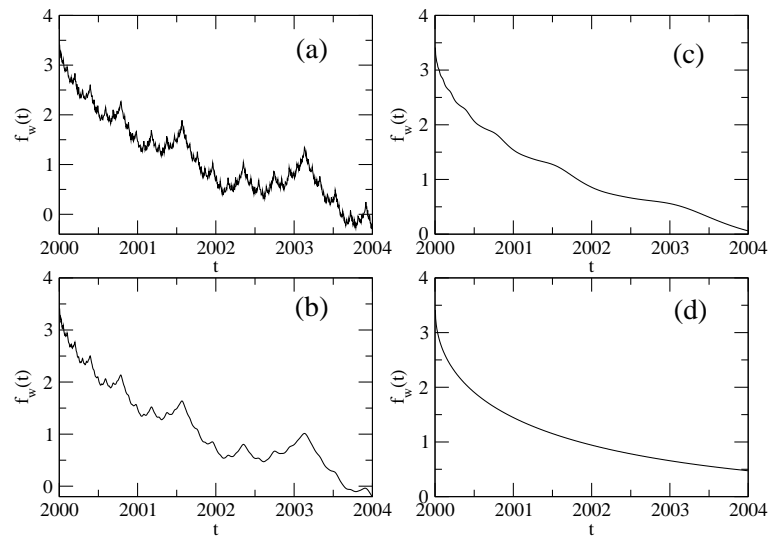


Figure 2.30: The Weierstrass-type function of Eq. (2.12) for (a)  $\gamma = \pi/2$ , (b)  $\gamma = 0.93\pi/2$ , (c)  $\gamma = 0.90\pi/2$  and (d)  $\gamma = 0$ . For all the plots  $D = 1.5$  and  $\lambda = 2$ . The sum in Eq. (2.12) has been truncated at  $N = 32$  because the function does not change significantly beyond this value of  $N$ . The time axis has been rescaled, as the Weierstrass-type function is defined only for  $t \in [0, 1]$ . In the present plots the function is fractal only in (a).

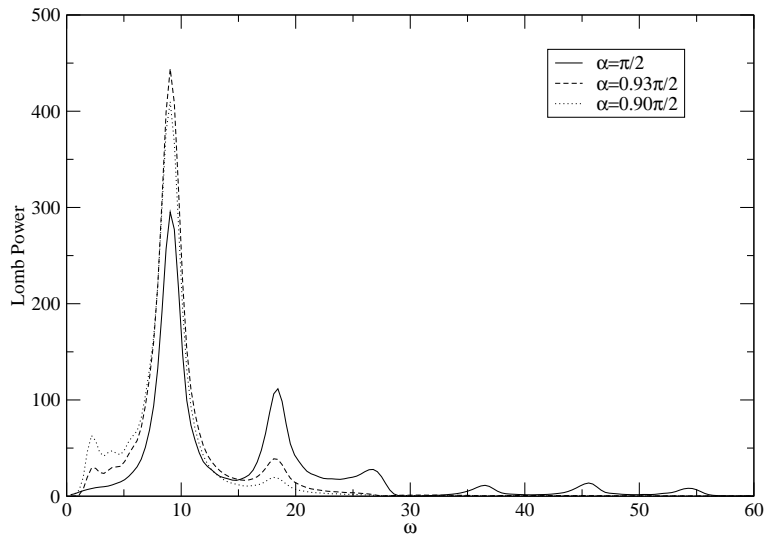


Figure 2.31: Lomb analysis for the Weierstrass-type function of Eq.(2.12). The self-similarity of the function in the fractal case ( $\gamma = \pi/2$ ) is reflected in the regularity of the high order harmonics. Once we smooth the function, the high order harmonics related to the fractality disappear while the dominant frequency of the log-periodic leading term is unaltered.